

APRIL limits atherosclerosis by binding to heparan sulfate proteoglycans.

Tsiantoulas D, Eslami M, Obermayer G, Clement M, Smeets D, Mayer FJ, Kiss MG, Enders L, Weißer J, Göderle L, Lambert J, Frommlet F, Mueller A, Hendrikx T, Ozsvar-Kozma M, Porsch F, Willen L, Afonyushkin T, Murphy JE, Fogelstrand P, Donzé O, Pasterkamp G, Hoke M, Kubicek S, Jørgensen HF, Danchin N, Tabassome S, Scharnagl H, März W, Borén J, Hess H, Mallat Z, Schneider P, Binder C

Nature 597, 92-96.

doi.org/10.1038/s41586-021-03818-3

Publisher's web site: <https://www.nature.com/articles/s41586-021-03818-3>

1 APRIL limits atherosclerosis via binding to heparan sulfate proteoglycans

2
3 Dimitrios Tsiantoulas^{1*}, Mahya Eslami², Georg Obermayer^{1,3}, Marc Clement⁴, Diede Smeets¹,
4 Florian J. Mayer¹, Máté G. Kiss^{1,3}, Lennart Enders³, Juliane Weißer³, Laura Göderle^{1,3}, Jordi
5 Lambert⁴, Florian Frommlet⁵, André Mueller³, Tim Hendrikx¹, Maria Ozsvar-Kozma^{1,3}, Florentina
6 Porsch^{1,3}, Laure Willen², Taras Afonyushkin^{1,3}, Jane E. Murphy⁴, Per Fogelstrand⁶, Olivier
7 Donzé⁷, Gerard Pasterkamp⁸, Matthias Hoke⁹, Stefan Kubicek³, Helle F. Jørgensen⁴, Nicolas
8 Danchin¹⁰, Tabassome Simon^{11,12}, Hubert Scharnagl¹³, Winfried März^{13,14}, Jan Borén⁶, Henry
9 Hess¹⁶, Ziad Mallat^{4,17§}, Pascal Schneider^{2§}, Christoph J. Binder^{1,3*}

10
11 ¹Dept. of Laboratory Medicine, Medical University of Vienna, Vienna, 1090, Austria

12 ²Department of Biochemistry, University of Lausanne, Epalinges, CH-1066, Switzerland

13 ³CeMM Research Center for Molecular Medicine of the Austrian Academy of Sciences, Vienna, 1090, Austria

14 ⁴Division of Cardiovascular Medicine, Department of Medicine, University of Cambridge, Cambridge, CB2
15 OSZ, UK

16 ⁵Center for Medical Statistics, Informatics and Intelligent Systems, Medical University of Vienna, Vienna, 1090,
17 Austria

18 ⁶Institute of Medicine, University of Gothenburg, Göteborg, 40530, Sweden

19 ⁷Adipogen Life Sciences, CH-1066 Epalinges, Switzerland

20 ⁸University Medical Center Utrecht, 3584 CX Utrecht, Netherlands

21 ⁹Department of Internal Medicine II, Medical University of Vienna, Vienna, 1090, Austria

22 ¹⁰Assistance Publique-Hôpitaux de Paris (AP-HP), Hôpital Européen Georges Pompidou, Department of
23 Cardiology, 75015 Paris, France; Université de Paris, 75006 Paris, France

24 ¹¹AP-HP, Hôpital Saint Antoine, Department of Clinical Pharmacology and Clinical Research Platform of East
25 of Paris (URCEST-CRB-CRC), 75012 Paris, France

26 ¹²Sorbonne-Université (UPMC-Paris 06), 75012 Paris, France

27 ¹³Clinical Institute of Medical and Chemical Laboratory Diagnostics, Medical University of Graz, A-8036
28 Graz, Austria

29 ¹⁴Medical Clinic V, Medical Faculty Mannheim, University of Heidelberg, D-68167 Mannheim, Germany

30 ¹⁵Synlab Holding Deutschland GmbH, 86156 Augsburg, Germany

31 ¹⁶Translational Innovation Platform Immunology, Merck KGaA, Darmstadt, 64293, Germany

32 ¹⁷Université de Paris and INSERM U970, Paris Cardiovascular Research Center, Paris, France

33 § these authors contributed equally

42 **SUMMARY**

43 Atherosclerotic cardiovascular disease (CVD) is the leading cause of mortality worldwide^{1,2}.
44 Atherosclerotic plaque formation is initiated upon trapping of low-density lipoprotein (LDL) in
45 the subendothelial space of large and medium size arteries that initially involves binding of LDL
46 to heparan-sulfate proteoglycans (HSPGs)³, followed by a chronic inflammation and remodelling
47 of the artery wall³. A Proliferation Inducing Ligand (APRIL), a cytokine produced by many cell
48 types, binds to HSPGs⁴, but the physiology of this interaction is largely unknown. Here, we show
49 that genetic ablation or antibody-mediated depletion of APRIL aggravates atherosclerosis in mice.
50 Mechanistically, we demonstrate that APRIL confers atheroprotection via binding to heparan
51 sulfate (HS) chains of heparan-sulfate proteoglycan 2 (HSPG2), which limits LDL retention,
52 macrophage accumulation and necrotic core formation. Indeed, antibody-mediated depletion of
53 APRIL in mice expressing HS-deficient HSPG2 had no effect on atherosclerosis development.
54 Consistent with these data, treatment with a specific anti-APRIL antibody that promotes the
55 binding of APRIL to HSPGs reduces experimental atherosclerosis. Furthermore, the serum levels
56 of a previously unknown form of human APRIL protein that binds to HSPGs, which we termed
57 non-canonical APRIL (nc-APRIL), are associated independently of traditional risk factors with
58 long term (10- to 12-year follow up) cardiovascular mortality in patients with atherosclerosis. Our
59 data reveal hitherto unknown properties of APRIL that have broad pathophysiological implications
60 for vascular homeostasis.

61

62

63

64 **MAIN TEXT**

65 APRIL is encoded by the tumour necrosis factor ligand superfamily member 13 gene (*Tnfrsf13*)
66 and is produced by myeloid cells and stromal cells⁵. APRIL is involved in antibody class switching
67⁶ and plasma cell survival^{7,8} in mice and humans through its binding to two receptors TACI
68 (transmembrane activator and CAML interactor) and BCMA (B cell maturation antigen),
69 respectively, with the same APRIL-binding site⁹. Patients with coronary artery disease have
70 increased APRIL levels in plasma compared to sex- and age-matched healthy individuals¹⁰,
71 however its role in atherosclerosis remains elusive.

72 To investigate the effect of APRIL in atherosclerosis, we generated LDL receptor-deficient mice
73 that lack APRIL (*Ldlr^{-/-}April^{-/-}*). *Ldlr^{-/-}April^{-/-}* mice fed an atherogenic diet developed increased
74 plaque size (Fig. 1a) in the aortic root despite similar body weight, cholesterol and triglyceride
75 levels in plasma (Fig. 1d and Extended Data fig. 1a) compared to their littermate controls.
76 Moreover, aortic root plaques of *Ldlr^{-/-}April^{-/-}* mice displayed enhanced necrotic core and acellular
77 area (Fig. 1b and Extended Data fig. 1b) and macrophage content (Fig. 1c). Smooth muscle cell
78 content (Extended Data fig. 1c) and collagen deposition (Extended Data fig. 1d) of plaques in the
79 aortic root, and plaque size in the thoraco-abdominal aorta were not affected (Extended Data fig.
80 1a). Notably, APRIL deficiency did not alter the numbers of splenic B cell (Fig. 1e), T cell
81 (Extended Data fig. 1e) and peritoneal B cell subsets (Extended Data fig. 1f) or the proportions of
82 circulating monocytes in peripheral blood (Extended Data fig. 1g). Besides total IgA, which was
83 moderately reduced (consistent with previous findings⁶), total IgM, IgG1, IgG2b, IgG2c and IgG3
84 levels in plasma were similar between *Ldlr^{-/-}April^{-/-}* and *Ldlr^{-/-}April^{+/+}* mice (Fig. 1f). These data
85 suggest that APRIL confers an atheroprotective effect, independently of circulating cholesterol
86 levels or B cell immunity.

87 Although TACI binds APRIL, it also binds with high affinity to the B cell activating factor (BAFF)
88¹¹, which mediates the atheroprotective effect of TACI signaling¹². Since BCMA has much higher
89 affinity for APRIL than for BAFF¹³, we investigated the role of BCMA in the atheroprotective
90 properties of APRIL. *Ldlr^{-/-}* mice lacking BCMA in the hematopoietic system (*Ldlr^{-/-}hem-Bcma^{-/-}*
91) (Extended Data fig. 2a) displayed similar plaque size in the aortic root and thoraco-abdominal
92 aorta compared with *Ldlr^{-/-}hem-Bcma^{+/+}* controls (Extended Data fig. 2b and Extended Data fig.
93 2c). Body weight (Extended Data fig. 2c), triglyceride (Extended Data fig. 2c) and total cholesterol
94 levels (Extended Data fig. 2d) in plasma were not different between the groups. In contrast to

95 APRIL-deficient mice, *Ldlr^{-/-}hem-Bcma^{-/-}* mice had increased splenic B cell numbers (Extended
96 Data fig. 2e) whereas T cell numbers were similar between *Ldlr^{-/-}hem-Bcma^{-/-}* mice and *Ldlr^{-/-}hem-
97 Bcma^{+/+}* controls (Extended Data fig. 2f). Peritoneal B-2 cells - in contrast to B-1 cells - were also
98 increased in *Ldlr^{-/-}Bcma^{-/-}* mice (Extended Data fig. 2g). Hematopoietic BCMA deletion also
99 altered immunoglobulin levels in plasma (Extended Data fig. 2h). All together, these data suggest
100 that the atheroprotective properties of APRIL are not dependent on BCMA signalling.

101 Next, we investigated whether APRIL mediates its atheroprotective effects locally within the
102 atherosclerotic plaque microenvironment. According to the Genotype-Tissue Expression (GTEx)
103 project ¹⁴, APRIL gene expression levels are particularly high in human healthy arteries (Extended
104 Data fig. 3a), which indicate that APRIL is produced in the arterial microenvironment. We show
105 that the *Tnfsf13* transcripts are present in intermediate to high levels within the total transcriptome
106 of isolated primary vascular smooth muscle cells from the aortic arch or thoracic aorta of healthy
107 mice (Extended Data fig. 3b) and remain stable even under cell culture conditions (Extended Data
108 fig. 3c). Similarly, we found that human umbilical artery smooth muscle cells also express *Tnfsf13*
109 and its expression is not affected by typical pro-atherogenic stimuli (Extended Data fig. 3d).

110 In line with these results, we found that in human atherosclerotic plaques from the Athero-Express
111 clinical study ¹⁵, APRIL protein content is approximately 0.5% of the total plaque protein amount
112 (Fig. 2a). To further explore the protective properties of APRIL in atheroma formation, we probed
113 APRIL in human carotid and coronary arteries with and without atherosclerosis. APRIL, which
114 was present in both carotid and coronary arteries (Fig. 2b), was particularly enriched at the
115 basement membrane of the vascular endothelial cell layer as well as on their cell surface in both
116 atherosclerotic and non-atherosclerotic specimens (Fig. 2c, d). Next, we found that both
117 recombinant mouse and human multimeric flag-tagged APRIL protein (thereafter referred to as
118 flag-APRIL) bind to human umbilical vein endothelial cells (HUVECs) and this was completely
119 abrogated in the presence of heparin (Extended Data Fig. 4a, b) showing that APRIL binds to the
120 endothelium via its heparan sulfate binding site ⁴. To identify the endothelial proteins interacting
121 with APRIL, we conducted an anti-flag pull-down assay with HUVECs treated with flag-APRIL
122 and flag-control constructs followed by protein identification by mass-spectrometry. We identified
123 heparan sulfate proteoglycan 2 (HSPG2 or Perlecan) as an interactor of APRIL (Extended Data
124 fig. 4c). HSPG2 is an essential and highly enriched component of basement membranes ¹⁶ and has
125 been shown to promote atherosclerotic plaque formation ^{17,18}. We validated the interaction of

126 APRIL and HSPG2 by ELISA using HSPG preparations isolated from mouse basement
127 membranes (Extended Data fig. 4d). Furthermore, we found that APRIL co-localised with HSPG2
128 in the subendothelial basement membrane of human arteries with (Pearson's Coefficient $r = 0.785$)
129 or without atherosclerosis (Pearson's Coefficient $r = 0.687$) (Fig. 2e). In addition, exogenously
130 added murine multimeric flag-APRIL to cryosections of mouse carotid artery (Extended Data fig.
131 4e) could bind preferentially to arterial areas that were enriched in HSPG2 and the binding of
132 APRIL to the artery wall was mediated exclusively via its HSPG-binding site as it was completely
133 inhibited when APRIL was pre-incubated with heparin (Extended Data fig. 4f). Furthermore, a
134 Surface Plasmon resonance (Biacore) analysis showed that both total human ($K_D = 0.24 \times 10^{-6}$ M)
135 and mouse APRIL ($K_D = 1.6 \times 10^{-6}$ M) bind with affinity to heparan sulfate (Extended Data fig. 4g).
136 To investigate whether APRIL mediates its atheroprotective effects via binding to HSPG2, we
137 treated Apolipoprotein E deficient mice, which express HSPG2 lacking heparan sulfate chains
138 (*Apoe*^{-/-} *Hspg2*^{d3}), and control mice with either a depleting mouse anti-mouse APRIL (clone 108;
139 Extended Data fig. 5a, b, c) or an isotype antibody for seven weeks, while the mice were fed an
140 atherogenic diet for the last six weeks of the study. In agreement with the proatherogenic role of
141 genetic deficiency of APRIL (Fig. 1), antibody-mediated depletion of APRIL increased
142 atherosclerosis in *Apoe*^{-/-} *Hspg2*^{wt}, while it had no effect in *Apoe*^{-/-} *Hspg2*^{d3} mice (Fig. 2f, g). Plasma
143 cholesterol levels were similar among all experimental groups (Fig. 2h). It has been previously
144 shown that regular chow diet-fed *Apoe*^{-/-} *Hspg2*^{d3} mice develop reduced atherosclerosis compared
145 to control mice¹⁸. Here, we extend these findings showing a similar result for *Apoe*^{-/-} *Hspg2*^{wt} and
146 *Apoe*^{-/-} *Hspg2*^{d3} mice (that received the isotype antibody) fed an atherogenic diet (Fig. 2f, g),
147 despite plasma cholesterol levels >1,000 mg/dL (Fig. 2h). These data reveal the mechanism by
148 which APRIL impacts atherosclerosis and highlight the importance of HSPGs in the pathogenesis
149 of atherosclerosis, even in conditions of extreme hypercholesterolemia.

150 An important function by which heparan-sulfate chains of HSPG2 exhibit their proatherogenic
151 effect is via facilitating the LDL retention in the subendothelial space¹⁸, which is a rate-limiting
152 step for the development of atherosclerotic plaques¹⁹. Pre-treatment of sections of a mouse carotid
153 artery with APRIL decreased arterial retention of native LDL (isolated from healthy human
154 donors), which was detected with an anti-ApoB antibody (Extended Data fig. 6a). We obtained
155 similar data using HEK293 wild-type cells (that are decorated with HSPGs), which were incubated
156 with human LDL in the presence of different amounts of recombinant human APRIL (Extended

157 Data fig. 6b). In vivo, we show that *Ldlr^{-/-}April^{-/-}* mice (described in Fig.1) display increased ApoB
158 content in their atherosclerotic plaques compared to the controls (Extended Data fig. 6c). Taken
159 together, these data show the HSPG-binding site of APRIL exhibits atheroprotective properties by
160 limiting LDL retention in the subendothelial space. However, HSPGs are also involved in other
161 biological processes that are implicated in atherogenesis, such as monocyte adhesion, smooth
162 muscle cell proliferation and matrix protein arrest^{20,21}, which could be modulated by APRIL. We
163 found that lesions of *Ldlr^{-/-}April^{-/-}* mice have increased macrophage content (Fig. 1c). While we
164 consider this to be a consequence of enhanced disease stage, an additional effect may be mediated
165 through direct impact of the APRIL-HSPGs interaction on immune cell adhesion and arrest. In
166 support of our findings that the protective effect of APRIL is exerted locally in the artery wall,
167 overexpression of human APRIL in T cells, does not alter plaque size in *Apoe^{-/-}* mice²².

168 We hypothesized that an intervention that preserves or promotes APRIL binding to HSPGs
169 while blocking its interaction with BCMA and TACI would be beneficial in atherosclerosis. First,
170 we tested a mouse TACI-Ig (a decoy TACI receptor that blocks the TACI/BCMA binding site of
171 APRIL²³). TACI-Ig did not affect atherosclerosis in *Apoe^{-/-}* mice fed an atherogenic diet (Fig. 3a,
172 b). It is important to note that TACI-Ig also targets BAFF, which we have recently shown to exhibit
173 an atheroprotective role in experimental atherosclerosis²⁴. In agreement with BAFF-depleting
174 activities²⁴, treatment with TACI-Ig led to a strong depletion of follicular and marginal zone B
175 cells in the spleen (Extended Data fig. 7a-c) and atheroprotective B-1 B cells²⁵⁻²⁷ in the peritoneum
176 (Extended Data fig. 7d, e), and to reduced levels of atheroprotective IgM antibodies^{28,29} in plasma
177 (Extended Data fig. 7f).

178 To target only APRIL, we treated *Apoe^{-/-}* mice with an anti-mouse APRIL antibody (clone Apyr-
179 1-1; Extended Data fig. 7a, b, c) that targets selectively the BCMA/TACI-binding site of APRIL
180²³ and simultaneously increases the binding to HSPGs (Fig. 3c) without affecting stability and
181 levels of APRIL in plasma in vivo (Extended Data fig. 7g). Notably, treatment with anti-APRIL
182 antibody did not affect B cell and IgM humoral responses besides a partial reduction of marginal
183 zone B cells (Extended Data fig. 7a-f). Furthermore, treatment with the anti-APRIL antibody
184 Apyr-1-1 (which was initiated two weeks prior to the onset of the atherogenic diet feeding) reduced
185 atherosclerosis in both aortic root and thoraco-abdominal aorta (Fig. 3a, b) without affecting
186 plasma cholesterol levels triglycerides or body weight (Extended Data fig. 7h).

187 By validating different ELISA systems for the detection of human APRIL, we discovered that
188 human serum contains an additional and previously unknown form of APRIL, thereafter termed
189 non-canonical (nc) APRIL. This was evidenced when APRIL was depleted from sera or from an
190 APRIL standard either with TACI-Ig, a known inhibitor of APRIL and BAFF that binds the
191 immune receptor (BCMA/TACI)-binding site of APRIL, or with an anti-APRIL antibody
192 (Aprily2) that recognizes APRIL by immunohistochemistry and Western blot (Fig. 2b-e, Fig. 4b).
193 Only TACI-Ig, but not Aprily2, could deplete the signal in an APRIL ELISA (ELISA 1).
194 Conversely, only the Aprily2 antibody, but not TACI-Ig, could deplete the signal in another
195 APRIL-specific ELISA (ELISA 2) (Fig. 4a, b, c). To confirm this, we performed additional
196 depletion experiments using different anti-human APRIL antibodies whose specificities for
197 APRIL protein were characterized by epitope mapping (Extended Data fig. 8a-g). We found that
198 APRIL detected in serum by ELISA 2 could be depleted by several monoclonal antibodies
199 (Aprily1,2,5,6,8) recognizing at least two different epitopes, without affecting the detection of the
200 canonical form of APRIL (c-APRIL) by ELISA 1 (Extended Data fig. 8h). Moreover, human
201 APRIL depletion in serum by antibodies (clones: Mahya1 and 110.6) and biologicals (Atacicept;
202 human TACI-Fc fusion protein) that are directed against c-APRIL did not affect the detection of
203 nc-APRIL by ELISA 2 (Extended Data fig. 8i). Thus, both ELISAs are specific but recognize
204 different forms of APRIL. Notably, ELISA 2 recognizes a non-canonical APRIL (nc-APRIL)
205 unable to bind the immune receptor TACI. However, both nc-APRIL and c-APRIL bind to
206 heparan-sulfates with equivalent affinities of $K_D = 6.3 \times 10^{-7}$ M and $K_D = 2.6 \times 10^{-7}$ M respectively
207 (Extended Data fig. 4g). Flag-tagged c-APRIL and nc-APRIL displayed markedly different sizes
208 upon gel filtration under native conditions. c-APRIL eluted as a trimer and nc-APRIL as a much
209 larger multimer (Extended Data fig. 8j-n). Furthermore, nc-APRIL and c-APRIL are encoded by
210 the same gene, as deletion of the TNFSF13 gene by CRISPR/Cas9 in U937 cells resulted in loss
211 of both nc-APRIL and c-APRIL proteins in the supernatant (Extended Data fig. 8o, p). In addition,
212 both nc-APRIL and c-APRIL can be produced by the same transcript as transfection of 293T cells
213 with a plasmid containing a cDNA for wild-type Fc-hAPRIL led to the production of both nc-
214 APRIL and c-APRIL in the supernatant (Fig 4d, e). We then characterized purified human
215 recombinant non-canonical and canonical Fc-hAPRIL by “bottom-up” MS-based proteomics and
216 found two different C-terminal tryptic peptides, an abundant one from which the C-terminal
217 leucine residue was released by trypsin, and a minor one in which the C-terminal leucine was still

218 attached. While most tryptic peptide fragments were equally abundant for c-APRIL and nc-APRIL
219 the miscleaved fragment was not detectable in nc-APRIL by high-sensitivity targeted parallel
220 reaction monitoring, suggesting that the C-terminus of nc-APRIL might have already been
221 truncated (Extended Data fig. 9a-c). As the C-terminus of APRIL is structurally important
222 (Extended Data fig. 9d), we investigated the effect of C-terminal amino acid truncations in
223 determining the ratio of c-APRIL to nc-APRIL. To examine this, Fc-APRIL with a C-terminal
224 truncation of 1 amino acid (-1C) was transfected in 293T cells and led to the exclusive production
225 of nc-APRIL in the supernatant, while the more abundantly produced wild-type Fc-APRIL
226 contained both c- and nc-APRIL (Fig. 4d, e). Similar data were obtained with C-terminal
227 truncations of 2, 3, or 4 amino acids (Fig. 4d, e). Nc-APRIL proteins that were produced upon
228 truncations of 1, 2, 3, or 4 amino acids also failed to bind the receptor BCMA (Fig. 4f), which is
229 consistent with nc-APRIL lacking the binding site to TACI and BCMA. We also confirmed in
230 additional human samples that both nc- and c-APRIL exist in human serum, with nc-APRIL
231 present at higher levels compared to c-APRIL (Fig. 4g and Supplemental fig. 1). Taken together,
232 these data indicate that different forms of APRIL exist *in vivo* that may have distinct roles in health
233 and disease. In addition, as c-APRIL and nc-APRIL could be also formed from the same wild-type
234 amino acid sequence, it raises the hypothesis that APRIL may belong to the group of metamorphic
235 protein, which are protein that switch between different folding states ³⁰.

236 To examine a potential role of APRIL in human atherosclerotic CVD, we quantified serum nc-
237 APRIL and c-APRIL levels in 785 individuals with neurologically asymptomatic carotid
238 atherosclerosis that were enrolled in the prospective clinical ICARAS study ³¹ (Supplemental table
239 2). Kaplan-Meier analyses demonstrated a significant increase in cardiovascular mortality with
240 decreasing serum nc-APRIL levels (Fig. 4h). After adjustment for well-established cardiovascular
241 risk factors in the cox proportional hazard model, patients within the first tertile displayed a
242 significantly increased risk of all-cause mortality (Extended Data fig. 10a) and cardiovascular
243 mortality (Extended Data fig. 10a) compared with patients within the third tertile. In contrast,
244 serum c-APRIL levels were not associated with cardiovascular or all-cause mortality (Extended
245 Data fig. 10b). Next, we quantified nc-APRIL levels in the serum of 1,514 patients with
246 symptomatic and angiographically-documented coronary artery disease that were enrolled in the
247 LURIC prospective clinical study ³² (Supplemental table 3). Kaplan-Meier analyses demonstrated
248 a statistically significant increase in cardiovascular mortality with increasing serum nc-APRIL

249 levels in a 10-year follow-up (Fig. 4i), even after adjustment for multiple well-established
250 cardiovascular risk factors (Extended Data fig. 10c;). Similar results were obtained for all-cause
251 mortality (hazard ratio = 1.15, 95% confidence interval= 1.05 - 1.25, P = 0.002). Moreover, we
252 also show that high nc-APRIL levels in the serum of 974 patients with acute myocardial infarction
253 included in the FAST-MI clinical study ³³ are independently associated with death in a 2-year
254 follow-up (Extended Data fig. 10d). Taken together, we show that circulating nc-APRIL levels are
255 independently associated with cardiovascular mortality in three different clinical studies and
256 thereby provide epidemiological evidence for the relevance of APRIL in human atherosclerotic
257 CVD.

258 In conclusion, we show that APRIL confers atheroprotection via binding to heparan sulfates in the
259 arterial intima. It is likely that the stoichiometric relationship of this interaction may change and
260 be modulated by additional factors (such as chemokines reacting with HS-chains) with progression
261 of the disease. Future studies will investigate the therapeutic value of targeting APRIL in
262 atherosclerotic CVD.

263

264 REFERENCES:

- 265 1 World Health Organization. Global status report on noncommunicable diseases 2014. xvii,
266 280 pages (World Health Organization,, Geneva, Switzerland, 2014).
- 267 2. World Health Organization, Noncommunicable diseases country profiles 2018, ISBN: 978
268 92 4 151462 0. (2018).
- 269 3. Gistera, A. & Hansson, G.K. The immunology of atherosclerosis. *Nat Rev Nephrol* **13**,
270 368-380 (2017).
- 271 4. Ingold, K., *et al.* Identification of proteoglycans as the APRIL-specific binding partners. *J*
272 *Exp Med* **201**, 1375-1383 (2005).
- 273 5. Vincent, F.B., Morand, E.F., Schneider, P. & Mackay, F. The BAFF/APRIL system in SLE
274 pathogenesis. *Nat Rev Rheumatol* **10**, 365-373 (2014).
- 275 6. Castigli, E., *et al.* Impaired IgA class switching in APRIL-deficient mice. *Proc Natl Acad*
276 *Sci U S A* **101**, 3903-3908 (2004).
- 277 7. Huard, B., *et al.* APRIL secreted by neutrophils binds to heparan sulfate proteoglycans to
278 create plasma cell niches in human mucosa. *J Clin Invest* **118**, 2887-2895 (2008).
- 279 8. McCarron, M.J., Park, P.W. & Fooksman, D.R. CD138 mediates selection of mature
280 plasma cells by regulating their survival. *Blood* **129**, 2749-2759 (2017).
- 281 9. Hymowitz, S.G., *et al.* Structures of APRIL-receptor complexes: like BCMA, TACI
282 employs only a single cysteine-rich domain for high affinity ligand binding. *J Biol Chem*
283 **280**, 7218-7227 (2005).
- 284 10. Sandberg, W.J., *et al.* The tumour necrosis factor superfamily ligand APRIL (TNFSF13)
285 is released upon platelet activation and expressed in atherosclerosis. *Thromb Haemost* **102**,
286 704-710 (2009).

- 287 11. Mackay, F. & Schneider, P. Cracking the BAFF code. *Nat Rev Immunol* **9**, 491-502 (2009).
- 288 12. Tsiantoulas, D., *et al.* B Cell-Activating Factor Neutralization Aggravates Atherosclerosis.
- 289 *Circulation* **138**, 2263-2273 (2018).
- 290 13. Patel, D.R., *et al.* Engineering an APRIL-specific B cell maturation antigen. *J Biol Chem*
- 291 **279**, 16727-16735 (2004).
- 292 14. Consortium, G.T., *et al.* Genetic effects on gene expression across human tissues. *Nature*
- 293 **550**, 204-213 (2017).
- 294 15. Hellings, W.E., Moll, F.L., de Kleijn, D.P. & Pasterkamp, G. 10-years experience with the
- 295 Athero-Express study. *Cardiovasc Diagn Ther* **2**, 63-73 (2012).
- 296 16. Lord, M.S., *et al.* The multifaceted roles of perlecan in fibrosis. *Matrix Biol* **68-69**, 150-
- 297 166 (2018).
- 298 17. Vikramadithyan, R.K., *et al.* Atherosclerosis in perlecan heterozygous mice. *J Lipid Res*
- 299 **45**, 1806-1812 (2004).
- 300 18. Tran-Lundmark, K., *et al.* Heparan sulfate in perlecan promotes mouse atherosclerosis:
- 301 roles in lipid permeability, lipid retention, and smooth muscle cell proliferation. *Circ Res*
- 302 **103**, 43-52 (2008).
- 303 19. Skalen, K., *et al.* Subendothelial retention of atherogenic lipoproteins in early
- 304 atherosclerosis. *Nature* **417**, 750-754 (2002).
- 305 20. Sarrazin, S., Lamanna, W.C. & Esko, J.D. Heparan sulfate proteoglycans. *Cold Spring*
- 306 *Harb Perspect Biol* **3**(2011).
- 307 21. Parish, C.R. The role of heparan sulphate in inflammation. *Nat Rev Immunol* **6**, 633-643
- 308 (2006).
- 309 22. Bernelot Moens, S.J., *et al.* Impact of the B Cell Growth Factor APRIL on the Qualitative
- 310 and Immunological Characteristics of Atherosclerotic Plaques. *PLoS One* **11**, e0164690
- 311 (2016).
- 312 23. Haselmayer, P., Vigolo, M., Nys, J., Schneider, P. & Hess, H. A mouse model of systemic
- 313 lupus erythematosus responds better to soluble TACI than to soluble BAFFR, correlating
- 314 with depletion of plasma cells. *Eur J Immunol* **47**, 1075-1085 (2017).
- 315 24. Tsiantoulas, D., *et al.* BAFF Neutralization Aggravates Atherosclerosis. *Circulation*
- 316 (2018).
- 317 25. Kyaw, T., *et al.* B1a B lymphocytes are atheroprotective by secreting natural IgM that
- 318 increases IgM deposits and reduces necrotic cores in atherosclerotic lesions. *Circ Res* **109**,
- 319 830-840 (2011).
- 320 26. Gruber, S., *et al.* Sialic Acid-Binding Immunoglobulin-like Lectin G Promotes
- 321 Atherosclerosis and Liver Inflammation by Suppressing the Protective Functions of B-1
- 322 Cells. *Cell Rep* (2016).
- 323 27. Rosenfeld, S.M., *et al.* B-1b Cells Secrete Atheroprotective IgM and Attenuate
- 324 Atherosclerosis. *Circ Res* **117**, e28-39 (2015).
- 325 28. Lewis, M.J., *et al.* Immunoglobulin M is required for protection against atherosclerosis in
- 326 low-density lipoprotein receptor-deficient mice. *Circulation* **120**, 417-426 (2009).
- 327 29. Tsiantoulas, D., *et al.* Increased Plasma IgE Accelerate Atherosclerosis in Secreted IgM
- 328 Deficiency. *Circ Res* **120**, 78-84 (2017).
- 329 30. Dishman, A.F., *et al.* Evolution of fold switching in a metamorphic protein. *Science* **371**,
- 330 86-90 (2021).
- 331 31. Schillinger, M., *et al.* Inflammation and Carotid Artery--Risk for Atherosclerosis Study
- 332 (ICARAS). *Circulation* **111**, 2203-2209 (2005).

- 333 32. Winkelmann, B.R., *et al.* Rationale and design of the LURIC study--a resource for
334 functional genomics, pharmacogenomics and long-term prognosis of cardiovascular
335 disease. *Pharmacogenomics* **2**, S1-73 (2001).
- 336 33. Puymirat, E., *et al.* Acute Myocardial Infarction: Changes in Patient Characteristics,
337 Management, and 6-Month Outcomes Over a Period of 20 Years in the FAST-MI Program
338 (French Registry of Acute ST-Elevation or Non-ST-Elevation Myocardial Infarction) 1995
339 to 2015. *Circulation* **136**, 1908-1919 (2017).

340

341

342 **FIGURE LEGENDS**

343 **Figure 1. APRIL deficiency promotes atherosclerotic lesion formation in *Ldlr*^{-/-} mice.** *Ldlr*^{-/-}
344 *April*^{+/+} or *Ldlr*^{-/-}*April*^{-/-} mice were fed an atherogenic diet for 10 weeks. (a) Representative
345 photomicrographs of H&E-stained aortic root lesions (50x) and dot plot of the average lesion size
346 in the aortic origin expressed as $\mu\text{m}^2/\text{section}$ ($n = 9$ *Ldlr*^{-/-}*April*^{+/+} mice and $n = 12$ *Ldlr*^{-/-}*April*^{-/-}
347 mice; $P = 0.041$). (b) Dot plot showing the average percentage of the necrotic core size normalized
348 to lesion size ($n = 9$ *Ldlr*^{-/-}*April*^{+/+} mice and $n = 12$ *Ldlr*^{-/-}*April*^{-/-} mice; $P = 0.009$), (c)
349 Representative photomicrographs and dot plot showing the average percentage of the Mac-2⁺ area
350 normalized to DAPI⁺ area of the lesion ($n = 8$ *Ldlr*^{-/-}*April*^{+/+} mice and $n = 12$ *Ldlr*^{-/-}*April*^{-/-} mice;
351 $P = 0.047$). (d) Dot plot showing total plasma cholesterol ($n = 10$ *Ldlr*^{-/-}*April*^{+/+} mice and $n = 12$
352 *Ldlr*^{-/-}*April*^{-/-} mice). (e) Representative flow cytometry plots on B220⁺CD43⁻ gated cells and dot
353 plots of absolute numbers of follicular/transitional stage 2 (FO/T2), marginal zone (MZ,) CD21⁺
354 CD23⁻, transitional stage 1 (T1), newly formed (NF) and B-1 (defined as B220^{low} IgM⁺ CD43⁺) B
355 cells in the spleen ($n = 10$ *Ldlr*^{-/-}*April*^{+/+} mice and $n = 12$ *Ldlr*^{-/-}*April*^{-/-} mice). (f) Dot plots showing
356 the total IgM, IgG1, IgG2b, IgG2c, IgG3 and IgA plasma antibody titers ($n = 10$ *Ldlr*^{-/-}*April*^{+/+}
357 mice and $n = 12$ *Ldlr*^{-/-}*April*^{-/-} mice). All results show mean \pm s.e.m.. * $P < 0.05$, ** $P < 0.01$, (two-
358 tailed Mann-Whitney *U* or two-tailed unpaired Student *t* test), scale bar: 200 μm .

359

360 **Figure 2. APRIL protects from atherosclerosis via binding to heparan sulfate proteoglycan**
361 **2 (HSPG2).** (a) Dot plot showing the average amount of APRIL in total denatured protein lysates
362 of human atherosclerotic plaque extracts from the Athero-Express clinical study ($n=199$ samples)
363 (b) Representative photomicrographs of human carotid and coronary artery specimens stained with
364 an anti-APRIL antibody and analyzed by confocal microscopy. Representative photomicrographs
365 of different human coronary and carotid artery specimens with or without atherosclerosis stained

366 (c, d) with anti-APRIL and anti-CD31 antibodies and (e) stained with anti-APRIL, anti-CD31 and
367 anti-HSPG2 antibodies, and analyzed by confocal microscopy. (f, g, h) *Apoe*^{-/-}*Hspg2*^{wt} and *Apoe*^{-/-}
368 *Hspg2*^{d3} mice that were treated with either a mouse anti-mouse APRIL antibody (clone 108) or an
369 isotype IgG1 for 7 weeks and were fed an atherogenic diet for the last 6 weeks of the study. (f)
370 Representative photomicrographs of H&E-stained aortic root lesions and line graph of the total
371 lesion area in the aortic origin expressed as μm^2 (160 μm : P = 0.037, 240 μm : P = 0.004, 320 μm :
372 P = 0.045), (g) dot plot showing the average lesion size in the aortic origin expressed as
373 $\mu\text{m}^2/\text{section}$ (*Apoe*^{-/-}*Hspg2*^{wt} treated with 108 vs *Apoe*^{-/-}*Hspg2*^{wt} treated with isotype: P = 0.026,
374 *Apoe*^{-/-}*Hspg2*^{wt} treated with isotype vs *Apoe*^{-/-}*Hspg2*^{d3} treated with isotype: P = 0.028) and (h) total
375 plasma cholesterol. (f, g, h) All results show mean \pm s.e.m. of n = 11 *Apoe*^{-/-}*Hspg2*^{wt} treated with
376 108, n = 10 *Apoe*^{-/-}*Hspg2*^{wt} treated with isotype, n = 12 *Apoe*^{-/-}*Hspg2*^{d3} treated with 108 and n = 11
377 *Apoe*^{-/-}*Hspg2*^{d3} treated with isotype. *P<0.05, **P<0.01, ***P<0.001, (1- Way ANOVA and
378 Tukey's test, 2-Way ANOVA and Sidak's test). scale bars: (b) carotid 1 and 3; 100 μm , carotid 2;
379 20 μm and coronary 50 μm , (c) 10 μm , (d) 5 μm , (e) 10 μm , (f) 200 μm .

380

381 **Figure 3. Antibody targeting of APRIL at the BCMA/TACI binding site reduces**
382 **atherosclerosis *in vivo*.** *Apoe*^{-/-} mice were treated biweekly for 10 weeks with a mixture consisting
383 of either mouse anti-APRIL antibody (Apyr-1-1) and Ctrl-Ig (α -APRIL group), or TACI-Ig and
384 isotype IgG2b (TACI-Ig group), or isotype IgG2b and Ctrl-Ig (Ctrl group) and were fed an
385 atherogenic diet for the last 8 weeks of the study. (a) Representative photomicrographs of H&E-
386 stained aortic root lesions and dot plot of the average lesion size in the aortic origin expressed as
387 $\mu\text{m}^2/\text{section}$ (n = 10 *Apoe*^{-/-}; Ctrl, n = 12 *Apoe*^{-/-}; TACI-Ig, n = 10 *Apoe*^{-/-}; α -APRIL; P = 0.025).
388 Scale bar: 200 μm (b) Representative photomicrographs of Sudan-VI stained aortas and dot plot
389 of the quantification of *en face* atherosclerotic lesion size expressed as percentage of total aortic
390 area (n = 9 *Apoe*^{-/-}; Ctrl, n = 12 *Apoe*^{-/-}; TACI-Ig, n = 10 *Apoe*^{-/-}; α -APRIL; P = 0.006). (c) HEK
391 293 wild-type cells were stained with Flag-ACRP-mAPRIL A88 (multimeric APRIL) that was
392 preincubated or not with mouse anti-APRIL antibody Apyr-1-1 or heparin and analyzed by flow
393 cytometry. The results show that APRIL binds to HEK 293 wt cells in a heparin-inhibitable manner
394 as expected for binding to heparan sulfate proteoglycans, and that Apyr-1-1 increases this binding.
395 Data are representative of two independent experiments performed in duplicates (error bars are

396 smaller than symbols). All results show mean \pm s.e.m.. *P<0.05, **P<0.01 (1- Way ANOVA and
397 Newman-Keuls test).

398

399 **Figure 4. Levels of a non-canonical form of APRIL (nc-APRIL) in serum predict**
400 **cardiovascular mortality in humans. (a)** APRIL standard of c-APRIL specific ELISA was
401 depleted twice with beads coupled to a recombinant APRIL receptor (TACI-Ig) or to a control
402 receptor (TNFR2-Ig), or with beads coupled to an anti-APRIL monoclonal antibody (Aprily2) or
403 to an isotype-matched control (mIgG1), in the indicated combinations. Unbound fractions were
404 measured for APRIL using nc-APRIL specific (right) or c-APRIL specific ELISA (left). **(b)**
405 Recombinant flag-APRIL in native or unfolded states was depleted once with the indicated bead
406 combinations. Unbound fractions were analyzed by anti-flag Western blot. **(c)** Human serum from
407 a healthy individual was depleted twice with the indicated combinations of beads, then analyzed
408 for APRIL content with nc-APRIL specific (right) or c-APRIL specific ELISA (left). **(d)** Fc-
409 human APRIL (wt) (aa 98-233) and Fc-APRIL with C-term truncations of 1, 2, 3, or 4 amino acids
410 were transfected in HEK-293T cells, and S/N and cell extracts were analyzed by reducing WB. **(e)**
411 Fc-APRIL with or without C-term truncations were measured with a c-APRIL specific (left) and
412 a nc-APRIL specific ELISA (right) at 25 ng/ml and 125 ng/ml respectively. **(f)** S/N adjusted for
413 APRIL concentrations were tested for activity on BCMA:Fas reporter cells. For mock, same
414 volume as truncated APRIL was used. **(g)** Quantified c-APRIL was used as a standard in the c-
415 APRIL specific ELISA (left) and quantified purified nc-APRIL was used as a standard in the nc-
416 APRIL specific ELISA (middle). Using these standard curves, the concentration of c-APRIL and
417 nc-APRIL was measured by ELISA in sera of healthy individuals (n = 8, two-tailed paired Student
418 *t* test, P <0.001). Serum levels of nc-APRIL were associated with cardiovascular mortality in **(h)**
419 asymptomatic individuals included in the ICARAS study and **(i)** in symptomatic patients included
420 in the LURIC. Data are representative of **(a, b, c, e)** three and **(d, g)** two independent experiments.
421 **(a, c, e, g)** Results show mean \pm s.e.m. **(h, i)** see methods for the methodology of statistical
422 analysis.

423

424 **METHODS**

425 **Mice, treatments and diets**

426 *Ldlr*^{-/-} and *ApoE*^{-/-} mice were bought from The Jackson Laboratories (USA). *April*^{-/-} mice were
427 provided by Genentech (USA). *Bcma*^{-/-} mice were provided by Biogen (USA). *Ldlr*^{-/-}*April*^{-/-} mice
428 were generated by crossing *Ldlr*^{-/-} and *April*^{-/-} mice. *Hspg2*^{d3} sperm was purchased from the
429 Biocenter Oulu (University of Oulu) and mice were generated via in vitro fertilization of *ApoE*^{-/-}
430 mice. All mice were on C57BL/6J background and were maintained either in the SPF facility of
431 the Medical University of Vienna (Austria) or of the University of Lausanne. Female *Ldlr*^{-/-}*April*
432 ^{-/-} and *Ldlr*^{-/-}*April*^{+/+} littermate mice (13-15 weeks old) were fed an atherogenic diet (0.2%
433 cholesterol, 21% fat; E15721-347 bought from Ssniff, Germany) for 10 weeks. For bone marrow
434 transplant experiments, male *Ldlr*^{-/-} mice (10 weeks old) were irradiated (10.5 Gray) then
435 reconstituted by i.v. injection with 7 x 10⁶ bone marrow cells isolated from *Bcma*^{+/+} and *Bcma*^{-/-}
436 donors. All mice could recover for four weeks and then they were placed on atherogenic diet for
437 10 weeks. Female *ApoE*^{-/-} mice (8 weeks old) were injected biweekly for 10 weeks with 5 mg/kg
438 of a mixture consisting of either mouse anti-APRIL antibody (Apyr-1-1; AG-27B-0001PF,
439 purchased from Adipogen, Liestal, Switzerland) and Ctrl-Ig, or TACI-Ig and isotype IgG2b
440 (LEAF; Biolegend), or isotype IgG2b and Ctrl-Ig (all reagents were provided by Merck KGaA,
441 Germany). In addition, all *ApoE*^{-/-} mice were fed an atherogenic diet for the last 8 weeks of the
442 study. Female littermate *ApoE*^{-/-}*Hspg2*^{wt} (data from *ApoE*^{-/-} *Hspg2*^{wt/wt} and *ApoE*^{-/-} *Hspg2*^{wt/d3} mice
443 were pooled because no differences were observed between the two genotypes) and *ApoE*^{-/-}*Hspg2*^{d3}
444 mice (8 weeks old) were injected biweekly for 7 weeks with 5 mg/kg of either a blocking mouse
445 anti-mouse APRIL antibody (108; Extended Data fig. 5a-c; available from Adipogen under
446 Centotto-1; AG-20B-0083) or an isotype IgG1 (Ultra LEAF; Biolegend), and mice were fed an
447 atherogenic diet for the last 6 weeks of the study.

448 Multimeric human and mouse flag-ACRP30-APRIL fusion proteins (referred to as flag-APRIL)
449 were from Adipogen (human: AG-40B-0017-C010, mouse: AG-40B-0089-C010). Wild-type
450 C57BL/6J mice were injected intraperitoneally in Dulbecco's PBS (DPBS) with either 1 µg of
451 mouse multimeric flag-APRIL (Adipogen) or a mixture of 1 µg flag-APRIL and 10 µg mouse anti-
452 APRIL antibody (Apyr-1-1, AG-27B-0001PF, Adipogen). Blood was collected one, three, and six
453 hours later and flag-APRIL was quantified as described below.

454 Mice were matched for sex and age in all studies. All experimental studies were approved by the
455 Animal Ethics Committee of the Medical University of Vienna (Austria) 66.009/0281-
456 /WFV/3b/2014, 66.009/0223-WF/II/3b/2014 and 66.009/0398-V/3b/2019 or have been regulated
457 under the Animals (Scientific Procedures) Act 1986 Amendment Regulations 2012 following
458 ethical review by the University of Cambridge Animal Welfare and Ethical Review Body (PPL
459 PA4BDF775).

460

461 **Anti-APRIL antibodies and biologicals**

462 Anti-hAPRIL antibodies Mahya-1 (mouse IgG1, AG-20B-0078PF-C100), 110 (mouse IgG1) and
463 His-tagged BAFF 60-mer (AG-40B-0112-C010) were provided by Adipogen. Aprily1, Aprily2,
464 Aprily3, Aprily5, Aprily6, Aprily8, Aprily9 and Aprily10 (mouse IgG1) were custom-made by
465 NanoTools (Teningen, Germany). Anti-EDA antibody EctoD1 (mIgG1) was as described³⁴. The
466 hybridoma for anti-rat SHH-5E1 (mouse IgG1) developed by T.M. Jessell and S. Brenner-Morton
467 was obtained from the Developmental Studies Hybridoma Bank, maintained at the University of
468 Iowa. Atacicept (TACI-Fc) was provided by Merck (KGaA). Etanercept (TNFR2-Fc) was
469 purchased from the pharmacy of Lausanne University Hospital (CHUV). Bovine serum albumin
470 was from Thermo Scientific (Cat# 23209).

471

472 **Quantification of size, necrotic core and collagen content of atherosclerotic lesions**

473 Atherosclerotic lesion size (staining Hematoxylin and Eosin), necrotic core content (staining
474 Hematoxylin and Eosin or DAPI) and collagen content (staining with Sirius Red) were evaluated
475 by computer-assisted image analysis using Adobe Photoshop Elements 6.0 and Fiji software in
476 aortic root cross paraffin-embedded (n=9/mouse) or OCT-preserved sections (n=6/mouse) with 50
477 or 80 μm distance that were collected starting with the appearance of all 3 valve leaflets as
478 described previously¹².

479

480 **Quantification of total cholesterol and triglycerides in mouse plasma**

481 EDTA blood was collected from the vena cava at the time of sacrifice in MiniCollect purple cap
482 TUBE (Greiner Bio-One). Blood was centrifuged at 1000 g for 30 min at room temperature.
483 Plasma total cholesterol and triglycerides were measured in an ISO 15189 accredited medical

484 laboratory on Beckman Coulter AU5400 (Beckman Coulter) or Roche Cobas 8000 (Roche)
485 instruments.

486

487 **Flow cytometry**

488 Flow cytometry analysis of splenic and peritoneal B cell subsets was performed as described
489 previously^{24,35} using directly conjugated antibodies on single cell suspensions of freshly isolated
490 spleens and peritoneal cells. Splenic T cells were identified using anti-CD3 PE (clone 145-2C11;
491 eBiosciences), anti-CD4 FITC (clone GK1.5; eBiosciences), anti-CD8 APC (clone 53-6.7;
492 eBiosciences). Peripheral blood from the vena cava was diluted with PBS + 2% dextran (Sigma)
493 and incubated for at least 30 min at 37°C to concentrate the RBCs at the bottom of the tube. The
494 upper clear phase was collected, and cells were incubated with blocking anti-CD16/32 antibody
495 (clone 93; eBiosciences). Peripheral monocytes were identified by staining with anti-CD11b-APC
496 (clone M1/70; eBiosciences), anti-Ly6C-FITC (clone HK1.4; Biolegend) and anti-Ly6G-PE
497 (clone 1A8; Biolegend) as described previously²⁴.

498 HUVECs were stained in DPBS (Sigma) supplemented with 10% FBS (Gibco) with 0.5 µg/ml of
499 either murine flag-tagged APRIL⁴ or amino-terminal flag-tagged bacterial alkaline phosphatase
500 (BAP) fusion protein (Sigma) for 30 min at 4°C, followed by staining with 1 µg/ml of anti-flag
501 M2 antibody (Sigma) for 20 min at 4°C. Then cells were stained with 1 µg/ml of a biotinylated rat
502 anti-mouse IgG1 (clone A85-1; BD Biosciences) for 20 min at 4°C and streptavidin-APC
503 (eBiosciences) for 20 minutes at 4°C.

504 HEK 293 wild-type cells were stained for 20 min on ice with 50 µl of flag-ACRP-mAPRIL A88
505 (DYKDDDDKGGPGVQLH-[aa 18-111 of mACRP30]-LQ-[aa 88-232 of mAPRIL]) in FACS
506 buffer (PBS+ 5% FCS) at 1000 ng/ml final and 5-fold dilutions, either alone or after preincubation
507 with Apyr-1-1 at 25 µg/ml, or after preincubation with liquemine (DrossaPharm, Basel,
508 Switzerland) at 10 IU/ml final concentration. Then cells were stained with biotinylated anti-flag
509 M2 (1:500; Sigma F9291) followed by PE-coupled streptavidin (1:500; eBiosciences).

510 HEK 293 wild-type cells were stained with 5% rat serum in PBS+0.5% BSA (buffer) for 15 min
511 on ice. After washing with buffer, cells were incubated with 1, or 3 or 6 µg/ml of Fc-human
512 APRIL-A88 for 30 min on ice. After washing cells were incubated with human native LDL
513 (generated as described previously³⁶) at 25 or 75 or 225 µg/ml for 30 min on ice. Then, cells were
514 incubated with 4% PFA for 20 min at room temperature. After washing with buffer, cells were

515 stained with the monoclonal MB47 antibody (provided by Dr. Witztum's lab UCSD) at 0.5µg/ml
516 for 20 min on ice, followed by an anti-mIgG2a-biot (rat; clone R19-15; BD) for 15 min on ice and
517 PE-coupled streptavidin for 15 min on ice (1:400; eBiosciences). Data were acquired on a FACS
518 Calibur (BD) or FACS Accuri C6 (BD) or LSRFortessa (BD) and were analysed using Flow Jo
519 software 7.6 (Tree Star).

520

521 **Total antibody quantification in plasma by ELISA**

522 Total IgM, IgG1, IgG2b, IgG2c, IgG3 and IgA antibodies in plasma were measured by ELISA.
523 Briefly, 96-well white round-bottomed MicroFluor microtiter plates (Thermo Lab systems) or
524 immunoGrade, 96-well, PS Standard plates (781724; Brand) were coated with either an anti-mouse
525 IgM (Sigma; M8644; at 2 µg/ml) or anti-mouse IgG1 (Biolegend; RMG1-1; at 2 µg/ml) or anti-
526 mouse IgG2b (BD Biosciences; R9-91; at 3 µg/ml) or anti-mouse IgG2c (STAR135; at 1 µg/ml)
527 or anti-mouse IgG3 (BD Biosciences; R2-38; at 4 µg/ml) or anti-mouse IgA (BD Biosciences;
528 C10-3; at 3 µg/ml) in PBS overnight and then washed 3 times with PBS and blocked with Tris-
529 buffered saline containing 1% BSA (TBS/BSA) for 1 hour at room temperature. Then wells were
530 washed with either PBS (plates for IgM, IgG2b and IgG2c) or PBS supplemented with 0.05%
531 Tween (plates for IgG1, IgG3 and IgA), and diluted mouse plasma was added in TBS/BSA to the
532 wells and incubated overnight at 4°C. Plates were washed, and bound Igs were detected with either
533 an anti-mouse IgM antibody conjugated to alkaline phosphatase (Sigma; A9688), or the
534 biotinylated forms of anti-mouse IgG1 (BD Biosciences; A85-1) or anti-mouse IgG2b (BD
535 Biosciences; R12-3), or anti-mouse IgG2c (JIR 115-065-208) or anti-mouse IgG3 (BD
536 Biosciences; R40-82) or anti-mouse IgA (BD Biosciences; C10-1). Wells were washed again as
537 before and neutravidin conjugated to alkaline phosphatase was added where appropriate. Then,
538 wells were washed again as before and rinsed once with distilled water, and 25 µl of a 30%
539 LumiPhos Plus solution in dH₂O (Lumigen Inc) was added. After 75 min, the light emission was
540 measured with a Synergy 2 luminometer (BIO-TEK) and expressed as RLU per 100 ms.

541 For antibody isotyping, ELISA plates were coated with purified antibodies at 2 µg/ml in PBS,
542 blocked, and incubated with horse radish peroxidase-coupled anti-IgA (#1040-05), anti-IgM
543 (#1020-05), anti-IgG1 (#1070-05), anti-IgG2a (#1080-05), anti-IgG2b (#1090-05) or anti-IgG3
544 (#1100-05) (all from Southern Biotech) at 1:4000 in ELISA buffer for 1 hour at 37°C and developed

545 with *o*-phenylenediamine (OPD) - H₂O₂ substrate (Sigma-Aldrich, P9187). Reaction was terminated
546 with acid and plates were read at 492 nm.

547

548 **Flag-APRIL quantification by ELISA**

549 To quantify flag-APRIL in plasma, ELISA plates (maxi-sorp NUNC) were coated with 2 µg/ml in
550 70 µl final volume of an anti-flag antibody (Biolegend; clone L5) overnight at 4°C. Thereafter,
551 wells were blocked with PBS + 1% BSA for 1 hour at room temperature. Plasma samples were
552 added to the wells and incubated for 2 hours at room temperature. Bound flag-APRIL was detected
553 with a mouse anti-APRIL biotinylated antibody (clone 2C8; Extended Data fig. 5 a, b, d) used at
554 1 µg/ml and incubated for 1 hour at room temperature. Then streptavidin-HRP (R&D) was added
555 to the samples for 30 min at room temperature. Finally, 3,3',5,5' tetramethylbenzidine was added
556 for 15 min. Reaction was terminated with acid and optical density was measured at 450 nm in a
557 luminometer VICTOR X3 (PerkinElmer).

558 To quantify the interaction of APRIL with heparan sulfate proteoglycan 2 (HSPG2), ELISA plates
559 (maxi-sorp NUNC) were coated with 1 µg/ml of HSPGs from the basement membrane of
560 Engelbreth-Holm-Swarm mouse sarcoma (Sigma) overnight at 4°C. Thereafter, wells were
561 blocked with PBS + 1% BSA for 1 hour at room temperature and mouse multimeric flag-APRIL
562 (AG-40B-0089, Adipogen) was added at 1µg/ml for two hours at room temperature. Bound flag-
563 APRIL was detected with an anti-flag conjugated to FITC (Sigma, clone: M2). Fluorescence was
564 measured in a luminometer VICTOR X3 (PerkinElmer).

565

566 **Immunofluorescence analysis**

567 Primary HUVECs were cultured in EGM-2 Bullet kit Endothelial Cell Growth Medium without
568 heparin (Lonza) in chambered coverslips (Ibidi) until a confluent monolayer was formed. Then
569 cells were washed with PBS with Ca²⁺ once and fixed with 4% paraformaldehyde for 20 min. Then
570 cells were carefully washed three times with DPBS (Sigma) and were incubated with 50 mM
571 ammonium chloride for 10 min at room temperature. After washing as above cells were incubated
572 with 0.5 µg/ml of either human or murine multimeric flag-APRIL (Adipogen). For competition
573 experiments, staining with flag-APRIL was also performed in presence of 5 IU/ml heparin
574 (National Veterinary Services LTD, UK). An anti-flag antibody (clone: M2; Sigma) conjugated to
575 FITC was used to detect flag-APRIL.

576 Paraffin embedded sections of human coronary and carotid artery specimens with or without
577 atherosclerotic plaques obtained at necropsy and anonymized were provided by Dr. Patrick
578 Bruneval (Paris Transplant Group, France). Sections were rehydrated by incubation first in Xylene
579 (three times; each three minutes), then in ethanol (100%, 96%, 90% and 70%; each for three
580 minutes) and finally in dH₂O for three minutes. Then antigen retrieval (Dako) was performed for
581 1 hour in a water bath at 100°C. Sections were then permeabilized in 0.1% Triton + citric acid for
582 20 min and were blocked with 5% goat and/or donkey serum diluted in assay buffer (PBS +2 .5%
583 BSA + 2 mM EDTA + 0.01% sodium azide) for 30 min. Sections were then stained with a mouse
584 anti-human APRIL (Aprily-2), an anti-HSPG2 (clone: A7L6; Merck Millipore) and an anti-CD31
585 (clone: EPR3094; Abcam) in blocking buffer overnight at 4°C. Next, sections were stained with a
586 goat anti-rat AF488, goat anti-rabbit AF647 and goat anti-mouse AF555 or goat anti-mouse
587 AF488, donkey anti-rat AF555 and goat and anti-rabbit AF647 (all from Life Technologies) where
588 appropriate, in assay buffer for 3 hours at room temperature.

589 Paraffin embedded sections of mouse aortic root with atherosclerotic plaques rehydrated by
590 incubation first in Xylene (three times; each three min), then in ethanol (100%, 96%, 90% and
591 70%; each for three min) and finally in dH₂O for three min. Then antigen retrieval (Dako) was
592 performed for 1 hour in water-bath at 100°C. Sections were blocked with 5% donkey serum or a
593 mixture of 5% mouse serum and 2.5 µg/ml of anti-mouse CD16/32 antibody (clone 93; Invitrogen)
594 diluted in assay buffer (PBS + 2.5% BSA + 2 mM EDTA + 0.01% sodium azide) for 30 min.
595 Sections were then stained with either a rat anti-mouse Mac-2 (M3/38; Biolegend), or a rabbit
596 polyclonal anti-ApoB (ab20737; Abcam), or a mouse anti-aSMC antibody conjugated to Cy-3 in
597 blocking buffer overnight at 4°C. Next, sections were stained with either a donkey anti-rat AF488
598 or a donkey anti-rabbit AF555 (all from Life Technologies) in assay buffer for 3 hours at room
599 temperature.

600 For the LDL binding competition assay, cryosections (10 µm thickness) of a sham operated mouse
601 carotid artery from a model of neointima hyperplasia as described previously³⁷ were fixed in
602 acetone for 20 min at -20°C and then were incubated with 10 µg/ml of murine multimeric flag-
603 APRIL in assay buffer (PBS + 2.5% BSA + 2 mM EDTA + 0.01% sodium azide) or only with
604 assay buffer overnight at 4°C. After washing in DPBS (Sigma), sections were incubated with 100
605 µg/ml of human native LDL (isolated from healthy donors) for two hours at room temperature.
606 Sections were then fixed in 4% PFA for 15 min at room temperature and then blocked with 5%

607 donkey serum in assay buffer. Sections were then stained with a rabbit anti-ApoB antibody
608 (Abcam; ab20737) for 1.5 hours at room temperature and then with a donkey anti-rabbit conjugated
609 to AF555 (Life Technologies) for 1 hour at room temperature.

610 Mouse multimeric flag-APRIL was detected with an anti-flag PE (Biolegend; clone: L5) or a
611 mouse anti-mouse APRIL biotinylated antibody (clone: 2C8) and streptavidin PE (Biolegend) in
612 sections that were blocked with 5 µg/ml of anti-CD16/32 antibody (Thermo Fisher Scientific;
613 clone: 93). For competition experiments with heparin, flag-APRIL was mixed with 30 IU/ml
614 heparin (National Veterinary Services LTD, UK) prior to the addition on the section.

615 HSPG2 in murine carotid arteries was detected with an anti-HSPG2 antibody (clone: A7L6; Merck
616 Millipore) and donkey anti-rat AF555 (Life Technologies). Finally, all samples were stained with
617 Hoechst or DAPI solution for 8 min at room temperature. Epifluorescence or confocal microscopy
618 were performed using a Leica CTR6500 or Axio Imager M2 or Carl Zeiss LSM 700 (ZEISS) or
619 LSM780 (ZEISS) microscope and Zen software. The plugin JACoP in Fiji was used to calculate
620 the Pearson's Coefficient. The antibodies were used at 1- 6 µg/ml where appropriate.

621

622 **Coupling of proteins to Sepharose beads**

623 5 mg of TACI-Fc or TNFR2-Fc or 2 mg of Aprily1, Aprily2⁴, Aprily3, Aprily5, Aprily6, Aprily8,
624 Aprily9 or Aprily10 or EctoD1 antibodies or mouse IgG1 5E1 anti-rat SHH were coupled to 1 ml
625 of NHS-activated Sepharose beads (GE Healthcare, #90-1004-00). Briefly, beads stored in
626 isopropanol were centrifuged for 5 min at 2400g and washed three times with 1 ml of ice-cold 1
627 mM HCl. 1 ml of TACI-Fc or TNFR2-Fc at 5 mg/ml or Aprily or anti-rat SHH antibodies at 2
628 mg/ml in 0.2 M NaHCO₃, 0.5 M NaCl, pH 8.3 were added to the beads and incubated for 30 min
629 at room temperature. Beads were then washed three times with 1 ml of ethanolamine buffer (0.5
630 M ethanolamine, 0.5 M NaCl, pH 8.3) and then three times with 1 ml of acetate buffer (0.1 M
631 sodium acetate, 0.5 M NaCl, pH 4) and again 3 ml of ethanolamine buffer. Beads were incubated
632 for 30 min at room temperature in ethanolamine buffer, then washed three times with acetate
633 buffer, then ethanolamine buffer, then acetate buffer and finally PBS. Beads were stored in 1 ml
634 of PBS 0.05% azide at 4°C.

635

636 **Production and quantification of Flag-tagged or Fc-tagged APRIL**

637 Flag-hAPRIL, Flag-mAPRIL, Flag-mAPRIL (+Ala112) or Fc-hAPRIL with deletion or
638 truncations at the C-terminus were transiently transfected in 293T cells using PEI³⁸ in serum-free
639 OptiMEM medium in 10 cm plates. After seven days, the supernatants of Fc-tagged constructs
640 were collected, and the cells were washed in PBS and lysed in 200 µl of SDS containing lysis
641 buffer plus DTT and boiled for 5 min at 95°C to be loaded on a SDS-PAGE. Also, seven days after
642 the transfection, the supernatants of Flag-tagged APRIL constructs were affinity-purified on
643 TACI-Fc-Sepharose (see section “Coupling of proteins to Sepharose beads”), eluted with 50 mM
644 of Na-citrate pH 2.7 and immediately neutralized with Tris-HCl pH9. Buffer was exchanged for
645 PBS using a 30 kDa cut off centrifugal device (Millipore). Purified proteins were quantified by
646 absorbance at 280 nm using 1 mg/ml extinction coefficients of 0.857 and 1.092 for Flag-hAPRIL
647 and Flag-mAPRIL respectively. The concentration of Flag-hAPRIL was also determined by
648 densitometric quantification using the Fiji software³⁹ of Coomassie-blue-stained SDS-PAGE gels
649 using His-BAFF and bovine serum albumin (BSA) as standards. cAPRIL was produced by
650 affinity-purification of conditioned supernatants containing Flag-hAPRIL on TACI-Fc-Sepharose
651 beads, followed by depletion on Aprily2-Sepharose beads. Conversely, ncAPRIL was affinity
652 purified on Aprily2-Sepharose beads followed by depletion on TACI-Fc-Sepharose beads.
653 Denatured Flag-hAPRIL was prepared by mixing 1 µg of purified Flag-hAPRIL with 1 µl of
654 denaturation buffer from PNGase F kit (Biolabs, P0704S lot: 0431703) and 8 µl of H₂O and heated
655 for 10 min at 100°C. Then the mix was neutralized with 2 µl of 10% NP-40 and 2 µl of 10 x glyco-
656 buffer 2 from the same kit.

657

658 **Size exclusion chromatography**

659 100 ng of Adipogen APRIL (h) ELISA kit standard which was depleted either on TACI-Fc- or
660 Aprily2-Sepharose beads and their eluates were size-fractionated at a flow rate of 0.7 ml/min on a
661 Superdex S200 Increase HR 10/30 column (GE Healthcare) equilibrated in PBS, 10 µg/ml BSA,
662 with online absorbance monitoring at 280 nm and 1 ml fraction collection. Fractions were tested
663 in Adipogen and Invitrogen ELISA kits. The column was calibrated with 100 µl of a mixture of
664 the following proteins, each at 1.4 mg/ml, except ferritin at 0.14 mg/ml, with sizes of: 669
665 (thyroglobulin), 440 (ferritin), 158 (aldolase), 13.7 (ribonuclease A), all from GE Healthcare), 67
666 (bovine serum albumin), 43 (ovalbumin), 29 (carbonic anhydrase), and 6.5 kDa (aprotinin) (all
667 from Sigma-Aldrich).

668

669 **SDS-PAGE**

670 SDS-PAGE and western blot (using Aprily2 at 0.5 µg/ml) were performed under reducing
671 conditions according to standard procedures and revealed by WesternBright ECL spray
672 (Advansta). Coomassie blue staining was performed with a semidry iD Stain System
673 (Eurogentech).

674

675 **HEK 293T, Jurkat BCMA:Fas-2309 c113 and U937 cells**

676 HEK 293T and histiocytic lymphoma U937 cells were obtained from late Dr. Jürg Tschopp
677 (University of Lausanne). HEK 293T cells were cultured in DMEM plus 10% fetal calf serum.
678 Jurkat BCMA:Fas-2309 c113 cells were cultured in RPMI plus 10% fetal calf serum as reported
679 previously ⁴⁰. U937 cells and U937 cells deficient for BAFF were as described ⁴¹. U937 cells
680 deficient for APRIL or deficient for BAFF and APRIL were generated by lentiviral transduction
681 of a CRISPR/Cas9-expression vector carrying a hAPRIL gRNA as described, except that the
682 following annealed oligonucleotides were used for cloning (5'-
683 CACCGAGGATATGGTGTCCGAATCC-3' and 5'- AAACGGATTCGGACACCATATCCTC-
684 3')⁴¹. U937 cells were cultured in RPMI supplemented with 10% fetal calf serum.

685

686 **Human Umbilical Vein Endothelial Cell (HUVEC) culture**

687 Primary HUVECs were provided by Dr. Marion Gröger (Medical University of Vienna; Austria)
688 or Dr. Sanjay Sinha's group (University of Cambridge; UK). Cells were cultured in either EGM-
689 2 Bullet kit Endothelial Cell Growth Medium without heparin (Lonza) or 90% IMDM-Medium
690 supplemented with 10% FBS, 1% Glutamin, 1% Pen-Strep and 10ml LSGS (Gibco). Cells were
691 used up to the 5th passage.

692

693 **Human umbilical artery smooth muscle cells**

694 Human Umbilical artery smooth muscle cells were a gift of Dr. Peter Petzelbauer's lab (Medical
695 University of Vienna). Cells were cultured in Smooth Muscle Cell Growth Medium 2 (Promocell).
696 For gene expression analysis, cells were cultured in 24-well plate (ThermoFisher) until 80-90%
697 confluency and then were stimulated with either human TNF (eBiosciences) at 100ng/ml or native

698 human LDL at 50 µg/ml or CuOx-LDL at 50 µg/ml for 4 hours. Native human LDL and CuOx-
699 LDL were generated as described previously³⁶.

700
701 **Cytotoxicity assay**

702 Cytotoxicity assays using BCMA:Fas cells were performed as described⁴². Briefly, flat-bottomed
703 96 well plates with 3 to 4 × 10⁴ reporter cells per well in a final volume of 100 µl of RPMI plus
704 10% of fetal calf serum were used in the presence of the indicated concentrations of flag-hAPRIL
705 or Flag-mAPRIL, and 100 ng/ml of TACI-Fc, Apyr-1-1 or mAb 108. After an overnight incubation
706 at 37°C, 5% CO₂, cell viability was monitored with a colorimetric (PMS/MTS) test.

707
708 **Total RNA extraction, cDNA synthesis and Real-time PCR analysis**

709 Total RNA was extracted from cells with the peqGold total RNA kit (Peqlab) and cDNA was
710 synthesized using the High-capacity cDNA reverse transcription kit (Applied Biosystems).
711 Quantitative Real-time SYBR green based PCR (Peqlab) was performed with the KAPA SYBR
712 green FAST BioRad icycler kit (Peqlab) on a BioRad CFX96 Real-time system. *36B4* and *18S*
713 were used as reference genes. Data were analysed using the ddCT method.

714 **Primer list:**

715 *mouse Bcma* forward: 5- ATCTTCTTGGGGCTGACCTT-3
716 *mouse Bcma* reverse: 5- CTTTGAGGCTGGTCCTTCAG -3
717 *36B4* forward: 5-AGGGCGACCTGGAAGTCC-3
718 *36B4* reverse: 5-CCCACAATGAAGCATTGGA-3
719 *human Tnfsf13* forward: 5- ATGGGTCAGGTGGTGTCTCG-3
720 *human Tnfsf13* reverse: 5-TCCCCTTGGTGTAAATGGAAGA-3
721 *human il-6* forward: 5- CAGGAGAAGATTCCAAAGAT-3
722 *human il-6* reverse: 5- CTCTTGTTACATGTCTCCTT-3
723 *human 18S* forward: 5- GTAACCCGTTGAACCCATT-3
724 *human 18S* reverse: 5- CCATCCAATCGGTAGTAGCG-3

725
726 **RNA sequencing and data analysis**

727 Aortas were isolated from C57BL/6 males. For ex vivo samples, tissues were immediately
728 transferred to RNAlater followed by isolation of ascending aorta (AA) and descending thoracic
729 aorta (DT) segments before manual removal of the adventitial and endothelial cell layers. The
730 cleaned medial layer from 3-5 animals was then lysed in Trizol (Thermo-Fisher), RNA isolated
731 and cleaned on a RNeasy column (Qiagen). *In vitro* cultured VSMC samples were isolated from
732 enzymatically dispersed VSMCs that had been cultured for 4-5 passages in DMEM supplemented

733 with 10% fetal calf serum, glutamine and penicillin. Sequencing libraries were generated from 550
734 ng quality-assessed total RNA (RNA integrity number [RIN] 7.8-9) using the TruSeq Stranded
735 mRNA Library Prep Kit (Illumina) and sequenced using HiSeq (Illumina).
736 Data analysis: Raw sequencing reads were quality controlled using *FastQC v0.11.3*
737 (<https://www.bioinformatics.babraham.ac.uk/projects/fastqc/>) and trimmed using the *Trim Galore*
738 *v0.4.1* wrapper (https://www.bioinformatics.babraham.ac.uk/projects/trim_galore/). Reads were
739 then aligned to the GRCm38 mouse reference genome using *Tophat v2.0.12* (Trapnell et al 2009).
740 Reads with a minimum map quality of 20 were imported into *Seqmonk 1.45.4*
741 (<http://www.bioinformatics.babraham.ac.uk/projects/seqmonk>) for quantitation using the RNA-
742 seq quantitation pipeline, and visualisation. Data is available form GEO, GSE117963: from
743 VSMCs from the aortic arch and descending thoracic aorta and GSE17858 (from mouse
744 primary VSMCs that were stored in Trizol after isolation or had been cultured for 4-5 passages
745 until the analysis

746

747 **Surface Plasmon Resonance**

748 For the Biacore measurements, a Biacore X100 system was used. Biotinylated heparin at a
749 concentration of 1.5 µg/ml (Sigma-Aldrich B9806-10MG) was coupled to a Streptavidin Sensor
750 Chip SA (Cytiva BR100032) as the ligand, reaching a response of 152.2 RU. All measurements
751 were performed in PBS as general buffer. The different purified proteins (analytes) were tested in
752 single-cycle Kinetics/Affinity assay, preceded by a priming and a startup cycle with buffer. Protein
753 solutions were prepared as a 3x dilution series in PBS going down from 1000 nM
754 (1000/333/111/37/12.3 nM), with 70 sec contact time, 600 sec dissociation time, and 30 sec
755 regeneration contact time. The chip was regenerated using a 500 mM NaCl, 25 mM NaOH
756 solution. Results were analyzed using the Biacore X100 Evaluation software version 2.0.1 Plus
757 Package. Stable response was measured just before injection of the next higher concentration (150
758 sec after injection stop, time window 15 sec). K_D -values were calculated using the Steady State
759 affinity model. Values of the stable response at different concentrations were exported and plotted
760 as a binding curve using GraphPad Prism version 8.4.0 for Mac.

761

762 **Mass spectrometry – sample preparation**

763 HUVECs: HUVECs were cultivated in 10 cm dishes in 90% IMDM-Medium supplemented with
764 10% FBS, 1% Glutamine, 1% Pen-Strep and 10ml LSGS (Gibco) until they reached 90%
765 confluency. Then media was removed, and cells were stimulated (in duplicates) with 0.5 µg/ml of
766 either mouse flag-tagged APRIL⁴ or amino-terminal flag-tagged BAP protein (Sigma) as control
767 bait for 30 min at 37°C. At the end of the stimulation cells were washed three times with DPBS
768 (Sigma) and on-plate cell lysis was performed with immunoprecipitation buffer (50 mM Tris, 150
769 mM NaCl, 1% NP-40, 5 mM EDTA, 5 mM EGTA complemented with 5 mM PMSF and protease
770 inhibitor cocktail (Sigma)) for 20 min at 4 °C. Lysates were cleared of non-lysed particles by
771 centrifugation and protein concentration was determined by bicinchoninic acid (BCA) assay
772 (Pierce). 750 µg of each lysate were incubated with 20 µl of washed anti-flag M2 bead gel (Sigma)
773 and incubated for 4 hours at 4°C with gentle rotation. Supernatants were removed, and beads were
774 washed 3 times with TBS and proteins were eluted twice with 100 mM glycine pH 3.0 for 5 min
775 at RT. Eluates were neutralized by addition of TBS pH 7.4. After denaturation with NP-40 and
776 incubation at 95°C for 10 min, 1000 units of PNGase F (New England Biolabs) were added and
777 incubated at 37°C for 6 hours. Deglycosylated proteins were subjected to tryptic digestion using
778 the filter-aided sample preparation (FASP) protocol^{43,44}. In brief, proteins were reduced with DTT
779 and loaded onto 30 kDa molecular weight cut-off filter columns and washed with 8 M urea in 100
780 mM Tris. Reduced cysteine side chains were alkylated with 55 mM iodoacetamide for 30 min at
781 RT in the dark. Excessive reagent was removed by additional washing steps with 8 M urea in 100
782 mM Tris. The buffer was exchanged again by washing to 50 mM triethylammonium bicarbonate
783 and 1 µg of sequencing grade trypsin (Promega) was added to each filter. The digest was allowed
784 to proceed for 16 hours at 37°C. The resulting peptides were washed of the filters and desalted
785 using the stop-and-go extraction (STAGE) protocol⁴⁵. Desalted peptides were reconstituted in 5
786 % formic acid for LC-MSMS analysis.

787 Human APRIL: 10 µg (~10 µl) of purified canonical or non-canonical APRIL was resuspended in
788 50µL 8M urea in 100 mM TEAB buffer, pH 8 and proteins reduced with a final concentration of
789 10 mM DTT and incubated at 56°C for 1 hour. After cooling down to room temperature, reduced
790 cysteines were alkylated with iodoacetamide at a final concentration of 55 mM for 30 min in the
791 dark. Prior to tryptic digestion, urea concentration was diluted with 100 mM TEAB buffer pH 8 to
792 1.5 M and samples were digested with 1 µg of trypsin overnight at 37°C. Peptides were acidified
793 to a final concentration of 1% TFA and cleaned up by solid phase extraction using C18 SPE

794 columns (SUM SS18V, NEST group, USA) according to the manufacturer's instructions. Peptides
795 were eluted using two times 50 μ l 90% Acetonitrile, 0.4% formic acid, organic solvent removed
796 in a vacuum concentrator and dried samples reconstituted in 20 μ l of 0.1% TFA.

797

798 **1D-RP Liquid Chromatography Mass Spectrometry**

799 HUVECs: Liquid chromatography mass spectrometry was performed on a Q Exactive™ Hybrid
800 Quadrupole-Orbitrap (ThermoFisher Scientific, Waltham, MA) coupled to an Agilent 1200 HPLC
801 nanoflow system (Agilent Biotechnologies, Palo Alto, CA) via nanoelectrospray ion source using
802 a liquid junction (Proxeon, Odense, Denmark). Tryptic peptides were loaded onto a trap column
803 (Zorbax 300SB-C18 5 μ m, 5 \times 0.3 mm, Agilent Biotechnologies) at a flow rate of 45 μ L/min using
804 0.1% TFA as loading buffer. After loading, the trap column was switched in-line with a 75 μ m
805 inner diameter, 20 cm analytical column (packed in-house with ReproSil-Pur 120 C18-AQ, 3 μ m,
806 Dr. Maisch, Ammerbuch-Entringen, Germany). Mobile-phase A consisted of 0.4% formic acid in
807 water and Mobile-phase B of 90 % acetonitrile in water plus 0.4 % formic acid. The flow rate was
808 set to 250 nL/min and a 60 min gradient applied (4% to 24% solvent B within 30 min, 24% to 36%
809 solvent B within 4 min and, 36% to 100% solvent B within 1 min, 100% solvent B for 4 min before
810 equilibrating at 4% solvent B for 21 min). For the MS/MS experiment, the Q Exactive™ MS was
811 operated in a Top10 DDA mode with a MS1 scan range of 350 to 1,650 m/z at a resolution of
812 70,000 (at m/z of 200). Automatic gain control (AGC) was set to a target of 3 \times 10E6 and a
813 maximum injection time of 100 ms. MS2-spectra were acquired at a resolution of 17,500 (at m/z
814 of 200) with AGC settings of 1 \times 10E5 and a maximum injection time of 120 ms. Precursor
815 isolation width was set to 1.6 Da and the HCD normalized collision energy to 28%. The threshold
816 for selecting MS2 precursor ions was set to an underfill ratio of ~12%. Dynamic exclusion for
817 selected ions was 60 s. A single lock mass at m/z 445.120024 was employed for internal mass
818 calibration⁴⁶. All samples were analyzed in technical duplicates. XCalibur version 4.1.31.9 Tune
819 2.9.2926 were used to operate the Q Exactive MS instrument.

820 Human APRIL: Mass spectrometry was performed on an Orbitrap Fusion™ Lumos™ Tribrid™
821 mass spectrometer (Thermo Fisher Scientific, San Jose, CA) coupled to a Dionex U3000 RSLC
822 nano UHPLC system (Thermo Fisher Scientific, San Jose, CA) via nanoflex source interface
823 applying a hybrid approach consisting of an inclusion list triggered data dependent acquisition
824 (DDA) experiment followed by a parallel reaction monitoring (PRM) experiment. A preceding

825 DDA discovery shotgun LC-MS experiment was carried out to generate a scheduled mass list for
826 99 selected human Fc-APRIL derived high confidence (1%FDR) peptide sequences using
827 Proteome Discoverer 2.4. Approximately equal amounts of either canonical and non-canonical
828 APRIL tryptic peptides were loaded onto a trap column (Acclaim™ PepMap™ 100 C18, 3µm, 5
829 × 0.3 mm, Fisher Scientific, San Jose, CA) at a flow rate of 10 µL/min using 0.1% TFA as loading
830 buffer. After loading, the trap column was switched in-line with a 50 cm, 75 µm inner diameter
831 analytical column (Acclaim™ PepMap™ 100 C18, 2µm, Fisher Scientific, San Jose, CA)
832 thermostatted at 50°C. Mobile-phase A consisted of 0.4% formic acid in water and mobile-phase
833 B of 0.4% formic acid in a mix of 90% acetonitrile and 10% water. The flow rate was set to 230
834 nL/min and a 90 min gradient applied (4 to 24% solvent B within 82 min, 24 to 36% solvent B
835 within 8 min and, 36 to 100% solvent B within 1 min, 100% solvent B for 6 min before re-
836 equilibrating at 4% solvent B for 18 min). For the MS/MS (DDA) experiment, the MS was
837 operated in a 3 sec TopN dependent scan cycle mode with a MS1 scan range of 375 to 1,650 m/z
838 at a resolution of 120,000 (at m/z of 200). Automatic gain control (AGC) was set to a target value
839 of 2×10^5 and a maximum injection time of 80 msec. MS2 scans were acquired at a resolution
840 of 15,000 (at m/z of 200) with an AGC setting of 5×10^4 and a maximum injection time of 100
841 msec. Precursor isolation width was set to 1.6 Da and HCD normalized collision energy to 30%.
842 Additional parameters were: MIPS enabled for peptide selection, intensity threshold for selecting
843 precursor ions set to $1 \times 5E4$, charge state inclusion of 2-6 and dynamic exclusion for selected ions
844 set to 60 seconds and a targeted mass list filter (scheduled mass list of 99 m/z values). A single
845 lock mass at m/z 445.120024 was employed (1). Settings for PRM were quadrupole isolation
846 window m/z of 0.8, HCD fragmentation using 30% NCE, Orbitrap detection at a resolution of
847 15,000 (at m/z of 200) and a defined first mass of 120 m/z. Automatic gain control (AGC) was set
848 to a target of 5×10^4 and a maximum injection time of 50 msec. XCalibur version 4.3.73.11 and
849 Tune 3.3.2782.28 were used to operate the instrument.

850

851 **Mass spectrometry data analysis**

852 HUVECs: Raw files were searched against a human database (containing 42265 entries,
853 downloaded from swissprot on 30th Dec. 2016) using Mascot version 2.3.02 (Matrix Science,
854 London, UK) and Phenyx (GeneBio, Geneva, Switzerland) as search engines. Common
855 contaminating proteins such as porcine trypsin, were appended to the database. Mass tolerances

856 were set to 4 ppm and 0.025 Da for precursor and fragment ions, respectively. Cleavage specificity
857 was set to tryptic, however, one missed cleavage was allowed. Carbamidomethylation of cysteines
858 was set as a static modification and oxidation of methionines was considered as a dynamic
859 modification. A target-decoy search strategy was employed to ensure a false discovery rate of 1 %
860 on the protein level.

861 Human APRIL: Acquired raw data files were processed using Proteome Discoverer 2.4.1.15 SP1
862 for DDA experimental data or Skyline version 20.1.0.155 for PRM experimental data. Data base
863 search within PD 2.4 was done using the Sequest HT algorithm and Percolator validation software
864 node (V3.04) to remove false positives with strict filtering at a false discovery rate (FDR) of 1%
865 on PSM, peptide and protein level. Searches were performed with full tryptic digestion against the
866 human SwissProt database V2017.06 including a common contamination list with up to two
867 miscleavage sites. Oxidation (+15.9949Da) of methionine was set as variable modification, whilst
868 carbamidomethylation (+57.0214Da) of cysteine residues was set as fixed modification. Data was
869 searched with mass tolerances of ± 10 ppm and 0.025 Da on the precursor and fragment ions,
870 respectively. Results were filtered to include peptide spectrum matches (PSMs) with Sequest HT
871 cross-correlation factor (Xcorr) scores of ≥ 1 and high peptide confidence. For relative quantitative
872 comparison of 26 selected APRIL tryptic peptide sequences, Skyline analysis was performed for
873 canonical and non-canonical Fc-APRIL. The PD result file was utilized to build up a reference
874 spectral library for Skyline analysis. Product ion chromatograms were extracted using the
875 following Skyline settings: Spectrum library ion match tolerance of 0.1 m/z; method match
876 tolerance of 0.025 m/z; MS/MS filtering using targeted acquisition method at resolving power of
877 15,000 at m/z of 200. High-selectivity extraction was used for all matching scans. Integrated peak
878 abundance values for selected peptides were exported (Supplemental table 1).

879

880 **Human blood collection from healthy individuals**

881 Human blood was collected from fasted healthy volunteers via venipuncture of the antecubital
882 vein using 21G needles. Blood samples were collected into 9 ml serum or sodium citrate (3.8%)
883 containing collection tubes (VACUETTE® tubes, Greiner Bio-One) and centrifuged within 20
884 min of venipuncture twice for 10 min at 2,000 g at room temperature. All plasma and serum
885 samples were aliquoted in 1.5 ml or 2 ml microtubes and were stored at -80° C until further

886 analysis. Human blood collection was conducted under the approval of the Ethics Committee of
887 the Medical University of Vienna, Austria (EK Nr: 1845/2015).

888

889 **Human APRIL quantification**

890 Canonical APRIL (c-APRIL) in human serum was quantified with the APRIL (human) ELISA kit
891 (Adipogen, AG-45B-0012-KI01; referred to as ELISA 1 in the main text) and non-canonical
892 APRIL (nc-APRIL) with the APRIL Human ELISA kit (Invitrogen, BMS2008; referred to as
893 ELISA 2 in the main text), according to manufacturer's instructions. For ELISA validation, 100
894 μ l of normal human serum, or 100 μ l of Invitrogen APRIL standard at 12.5 ng/ml were depleted
895 overnight at 4°C with 20 μ l of a 50% slurry of Sepharose beads coupled to the indicated
896 combinations of Aprily2, TACI-Ig or control reagents, with agitation. Beads were spun, and
897 supernatants were depleted again with fresh beads. APRIL in supernatants was measured with the
898 Invitrogen ELISA (80 μ l) or with the Adipogen ELISA (10 μ l for sera, 2 μ l for standard). For
899 native and unfolded APRIL, 50 μ l at 5 μ g/ml were depleted overnight at 4°C with 30 μ l of a 50%
900 slurry of the indicated bead combinations, then beads were spun down and 15 μ l of supernatant
901 was analysed by Western blot according to standard procedures, revealed with Aprily2 at 0.5
902 μ g/ml, followed by horseradish peroxidase-coupled anti-mouse secondary antibody and ECL.
903 Total APRIL in total denatured protein extracts from human atherosclerotic plaques (n=199) from
904 the Athero-Express¹⁵ was quantified with the APRIL Human ELISA kit (Invitrogen, BMS2008).

905

906 **Patients from the LURIC prospective clinical study (The Ludwigshafen Risk and**
907 **Cardiovascular Health study)** ³², **the ICARAS (Inflammation and Carotid Artery-Risk for**
908 **Atherosclerosis Study)** ³¹ **and French registry of Acute ST elevation or non-ST-elevation**
909 **Myocardial Infarction clinical study (FAST-MI)** ³³.

910 ICARAS study: In this single-center study, 1268 consecutive patients who underwent duplex
911 ultrasound investigations of the extracranial carotid arteries were prospectively enrolled between
912 March 2002 and March 2003. Of these, 203 patients (16%) were lost to clinical follow-up and for
913 280 patients (22%) no serum sample for the measurement of APRIL levels was available, leaving
914 785 patients for the final analysis. The 483 patients who had to be excluded from analysis did not
915 differ significantly from the subjects who were included with respect to baseline and demographic
916 parameters (age, sex, frequency of risk factors for atherosclerosis, and cardiovascular

917 comorbidities; data not shown). The study cohort comprised 486 male patients (62.1%); the
918 median age was 69.0 (IQR 61 to 76). Demographic data and clinical characteristics of the 785
919 patients are given in Supplemental table 2. Study design, inclusion and exclusion criteria have
920 been published previously ^{31,47}. In brief, patients with atherosclerotic carotid artery disease, as
921 defined by the presence of non-stenotic plaques or atherosclerotic carotid narrowing of any degree,
922 who were neurologically asymptomatic at the time of screening, were enrolled. The indications
923 for performing carotid ultrasound investigation included carotid bruits, cardiovascular risk factors
924 and known atherosclerotic diseases of other vessel areas. Patients with a myocardial infarction
925 (MI), stroke, coronary intervention or peripheral vascular surgery during the preceding 6 months,
926 were excluded from the study. The rationale behind this was the assumption that acute
927 cardiovascular events may affect laboratory measures and rather reflect the severity of an acute
928 situation than chronic atherosclerosis. The study complied with the Declaration of Helsinki and
929 was approved by the review board and the institutional ethics committee of the Medical University
930 of Vienna. All patients gave their written informed consent.

931 LURIC study: The detailed study design, inclusion and exclusion criteria have been published
932 previously ³². We analyzed 1,514 samples that were randomly selected. Demographic data and
933 clinical characteristics of the 1,514 patients are given in Supplemental table 3.

934 FAST-MI study: The detailed study design, inclusion and exclusion criteria have been published
935 previously ³³. We analyzed 974 samples.

936

937 **Clinical and laboratory data for the ICARAS clinical study**

938 Every patient completed a detailed study questionnaire assessing the patient's medical history,
939 current medication, biometric data, and family history. Physical examination was assessed by a
940 trained physician with special attention to patients' cardiovascular risk factors and comorbidities.
941 All demographic and vital parameters were ascertained by two independent observers. Antecubital
942 venous blood samples were drawn and analyzed directly without freezing according to local
943 laboratory standard procedure. In addition, a secondary serum sample of each patient was drawn
944 at baseline visit and directly frozen at -80°C according to local standard procedures. Color-coded
945 duplex sonography examinations of carotid arteries at baseline visits were performed on an
946 Acuson128 XP10 with a 7.5-MHZ linear array probe (Acuson, Malvern, PA, USA). Treating
947 physicians and ultrasonographers were blinded for all laboratory values. Definitions of risk factors

948 and comorbidities were published previously^{31,47}. Cardiovascular and all-cause mortality were
949 assessed by searching the national death register for the specific cause of death (according to the
950 International Statistical Classification of Diseases and Related Health Problems, 10th Revision).
951 Only the specific cause of death (e.g. stroke) was used to categorize death as either all-cause or
952 cardiovascular death. In 43% of deaths, the underlying cause was assessed by autopsy. All
953 demographic and vital parameters were ascertained by two independent observers.

954

955 **Statistical analyses**

956 Statistical analyses were performed using Graph Pad Prism 8 (Graph Pad Software). Experimental
957 groups were compared using two tailed Student's unpaired or paired *t* or two tailed Mann-Whitney
958 *U* test as appropriate. To analyse multiple group data, 1-Way ANOVA test followed by Newman-
959 Keuls or Tukey's test, or 2-Way ANOVA test followed by Sidak's test were used. Data are
960 presented as mean \pm s.e.m.. A P value of <0.05 was considered significant. ICARAS clinical study:
961 Serum levels of APRIL or nc-APRIL were categorized in tertiles or quartiles (where indicated) to
962 obtain clinically useful measures for the effect sizes. Continuous data are presented as median and
963 interquartile range (range from the 25th to the 75th percentile). Discrete data are given as counts
964 and percentages. ANOVA (analysis of variance) and the χ^2 test were used for comparisons
965 between tertiles or quartiles, as appropriate. The log-rank test was used for comparison between
966 groups. Event-free survival probabilities were estimated using the Kaplan–Meier method.
967 Univariable and multivariable Cox proportional hazards models were applied to assess the
968 association between serum levels of APRIL or nc-APRIL and the occurrence of either all-cause or
969 cardiovascular death, including the following variables: age (years), sex (male/female), history of
970 myocardial infarction (binary), history of stroke (binary), peripheral arterial disease (binary), body
971 mass index (kg/m²), hypertension (binary), diabetes mellitus (binary), serum creatinine (mg/dL),
972 glycohemoglobin A1 (%), levels of triglycerides (mg/dL), total cholesterol levels (mg/dL), low
973 density lipoprotein cholesterol levels (mg/dL), high-sensitivity C-reactive protein (mg/dL),
974 ICAM-1 (ng/ml), VCAM-1 (ng/ml) and statin treatment (binary). The selection of the variables
975 was defined a priori and is based on current guidelines for cardiovascular risk prediction. All of
976 the variables listed above were included in every multivariable Cox proportional hazard model
977 used for this study. Results of the Cox models are presented as hazard ratios (HR; 95% confidence
978 interval [CI]). We assessed the overall model fit using Cox–Snell residuals. We also tested the

979 proportional hazard assumption for all covariates using Schoenfeld residuals (overall test) and the
980 scaled Schoenfeld residuals (variable-by-variable testing). A 2-sided P value of <0.05 was
981 considered significant. All calculations were performed with SPSS (version 20.0, SPSS Inc) for
982 Windows. LURIC clinical study: Survival analysis was performed considering the following
983 variables as potential risk factors: Serum levels of nc-APRIL, age (years), sex (male/female), body
984 mass index, history of myocardial infarction (no, one, more than one), history of stroke (binary),
985 peripheral arterial disease (binary), body mass index (kg/m²), hypertension (binary), Type II
986 diabetes mellitus (binary), peripheral vascular disease (binary), isolated systolic hypertension
987 (≥ 140 / < 90), C-reactive protein (mg/dL) > 0.01 (binary), glycosylated hemoglobin (%), serum
988 creatinine (mg/dL), levels of triglycerides (mg/dL), total cholesterol levels (mg/dL). Serum levels
989 of nc-APRIL were categorized in quartiles for descriptive purposes and for Kaplan-Meier curves.
990 Baseline characteristics for all variables are provided for the complete data set and stratified by the
991 nc-APRIL quartiles. Metric variables are presented as mean \pm 95% confidence intervals. For
992 discrete variables counts and percentages are given. ANOVA (analysis of variance) and the χ^2 test
993 were used for comparisons between quartiles to provide a quick overview of potential confounding
994 of risk factors with nc-APRIL. Multivariable Cox proportional hazards models were applied to
995 assess the association between the above listed risk factors and the occurrence of either all-cause
996 or cardiovascular death. Due to very strong right-skewness the laboratory parameters serum
997 creatinine, triglycerides and cholesterol as well as nc-APRIL were log-transformed. Again, no
998 model selection was performed, and the set of variables was defined a priori based on current
999 guidelines for cardiovascular risk prediction. Results of the Cox models are presented as hazard
1000 ratios (HR; 95% confidence interval [CI]). The proportional hazard assumption was tested for all
1001 covariates using Schoenfeld residuals (overall test) and the scaled Schoenfeld residuals (variable-
1002 by-variable testing). A 2-sided P value of <0.05 was considered significant. All calculations were
1003 performed with R version 3.6.0 (<https://www.R-project.org/>). Survival analysis was
1004 performed using the R packages *survival* (<https://CRAN.R-project.org/package=survival>)
1005 and *survminer* (<https://CRAN.R-project.org/package=survminer>). FAST-MI clinical
1006 study: The primary endpoint was all-cause death during 2 years of follow-up after the index
1007 myocardial infarction. A multivariable Cox proportional-hazards model was used to assess the
1008 independent prognostic value of variables with the primary endpoint. The multivariable model
1009 comprised age, sex, previous or current smoking, previous myocardial infarction, family history

1010 of coronary disease, history of hypertension, diabetes, renal failure, heart rate at admission, heart
1011 failure, Killip class, left ventricular ejection fraction, hospital management (including reperfusion
1012 therapy, statins, beta blockers, clopidogrel, diuretics, digitalis, heparin), troponin I and log CRP
1013 levels.

1014

1015 **METHODS REFERENCES:**

- 1016 34. Kowalczyk-Quintas, C., *et al.* Generation and characterization of function-blocking anti-
1017 ectodysplasin A (EDA) monoclonal antibodies that induce ectodermal dysplasia. *J Biol*
1018 *Chem* **289**, 4273-4285 (2014).
- 1019 35. Tsiantoulas, D., *et al.* Increased Plasma IgE Accelerate Atherosclerosis in Secreted IgM
1020 Deficiency. *Circ Res* (2016).
- 1021 36. Chou, M.Y., *et al.* Oxidation-specific epitopes are dominant targets of innate natural
1022 antibodies in mice and humans. *J Clin Invest* **119**, 1335-1349 (2009).
- 1023 37. Kijani, S., Vazquez, A.M., Levin, M., Boren, J. & Fogelstrand, P. Intimal hyperplasia
1024 induced by vascular intervention causes lipoprotein retention and accelerated
1025 atherosclerosis. *Physiol Rep* **5**(2017).
- 1026 38. Tom, R., Bisson, L. & Durocher, Y. Transfection of HEK293-EBNA1 Cells in Suspension
1027 with Linear PEI for Production of Recombinant Proteins. *CSH Protoc* **2008**, pdb prot4977
1028 (2008).
- 1029 39. Schindelin, J., *et al.* Fiji: an open-source platform for biological-image analysis. *Nat*
1030 *Methods* **9**, 676-682 (2012).
- 1031 40. Bossen, C., *et al.* TACI, unlike BAFF-R, is solely activated by oligomeric BAFF and
1032 APRIL to support survival of activated B cells and plasmablasts. *Blood* **111**, 1004-1012
1033 (2008).
- 1034 41. Kowalczyk-Quintas, C., *et al.* Inhibition of Membrane-Bound BAFF by the Anti-BAFF
1035 Antibody Belimumab. *Front Immunol* **9**, 2698 (2018).
- 1036 42. Schneider, P., Willen, L. & Smulski, C.R. Tools and techniques to study ligand-receptor
1037 interactions and receptor activation by TNF superfamily members. *Methods in enzymology*
1038 **545**, 103-125 (2014).
- 1039 43. Manza, L.L., Stamer, S.L., Ham, A.-J.L., Codreanu, S.G. & Liebler, D.C. Sample
1040 preparation and digestion for proteomic analyses using spin filters. *Proteomics* **5**, 1742-
1041 1745 (2005).
- 1042 44. Wisniewski, J.R., Zougman, A., Nagaraj, N. & Mann, M. Universal sample preparation
1043 method for proteome analysis. *Nat Meth* **6**, 359-362 (2009).
- 1044 45. Rappsilber, J., Ishihama, Y. & Mann, M. Stop and Go Extraction Tips for Matrix-Assisted
1045 Laser Desorption/Ionization, Nanoelectrospray, and LC/MS Sample Pretreatment in
1046 Proteomics. *Anal Chem* **75**, 663-670 (2003).
- 1047 46. Olsen, J.V., *et al.* Parts per Million Mass Accuracy on an Orbitrap Mass Spectrometer via
1048 Lock Mass Injection into a C-trap. *Mol Cell Proteomics* **4**, 2010-2021 (2005).
- 1049 47. Mayer, F.J., *et al.* Combined Effects of Inflammatory Status and Carotid Atherosclerosis:
1050 A 12-Year Follow-Up Study. *Stroke* **47**, 2952-2958 (2016).

1051

1052

1053 **DATA AVAILABILITY**

1054 The RNA sequencing datasets (from vascular smooth muscle cells) are available in the Gene
1055 Expression Omnibus with accession codes GSE117963 and GSE (*TO BE COMPLETED*
1056 *BEFORE PUBLICATION*). All other relevant data are available from the corresponding authors
1057 upon reasonable request. Source data of Figures 1, 2, 3, 4 and Extended Data figures 1, 2, 5, 6, 7
1058 and 8 are included within the paper. Supplemental Information is available for this paper.

1060 **CODE AVAILABILITY**

1061 For the clinical studies, the calculations were performed with SPSS (version 20.0, SPSS Inc) for
1062 Windows, R version 3.6.0 (<https://www.R-project.org/>), survival analysis was performed using the
1063 R packages survival (<https://CRAN.R-project.org/package=survival>) and survminer
1064 (<https://CRAN.R-project.org/package=survminer>). For analysis of mass-spectrometry data,
1065 acquired raw data files were processed using Proteome Discoverer 2.4.1.15 SP1 for DDA
1066 experimental data or Skyline version 20.1.0.155 for PRM experimental data or using Mascot
1067 version 2.3.02 (Matrix Science, London, UK) and Phenyx (GeneBio, Geneva, Switzerland) as
1068 search engines. RNA-Seq data were quality controlled using FastQC v0.11.3
1069 (<https://www.bioinformatics.babraham.ac.uk/projects/fastqc/>) and trimmed using the Trim Galore
1070 v0.4.1 wrapper (https://www.bioinformatics.babraham.ac.uk/projects/trim_galore/). Reads were
1071 aligned to the GRCm38 mouse reference genome using Tophat v2.0.12 (Trapnell et al 2009).
1072 Reads with a minimum map quality of 20 were imported into Seqmonk 1.45.4
1073 (<http://www.bioinformatics.babraham.ac.uk/projects/seqmonk>).

1075 **ACKNOWLEDGMENTS-FUNDING:** We are particularly thankful to Ms. Astrid Fabry and Ms.
1076 Tamara Wenko for their help with the in vivo experimental studies and to Mr. Christoph Friedl for
1077 his help with confocal microscopy. This work was supported by grants of the Austrian Science
1078 Fund (SFB F54), the European Union (FP7 VIA) and the Leducq Foundation (TNE-20CVD03) to
1079 CJB, and by grants of the European Research Area Network on Cardiovascular Diseases (I4647),
1080 the British Heart Foundation (RCAG/917) to DT. DT is also supported by the Austrian Science
1081 Fund (I4963). PS is supported by the Swiss National Science Foundation (31003A_176256,
1082 310030E_197000). ZM is supported by the British Heart Foundation (RCAM/104, RCAM-659,
1083 RRCAM.163), the British Heart Foundation Center for Research Excellence (RE/18/1/34212), the

1084 NIHR Cambridge Biomedical Research Centre (RG85315), the European Union (FP7 VIA;
1085 RCAG/430) and the European Research Council (ERC). TH is supported by a NWO Veni grant
1086 (91619012).

1087
1088 **AUTHOR CONTRIBUTIONS:** D.T. conceived and designed the study, performed most of the
1089 experiments, analyzed and interpreted data, and wrote the manuscript, M.E. and P.S. generated
1090 materials, performed experiments to characterize nc-APRIL and interpreted data, G.O., L.E., S.K.,
1091 L.W., T.A., T.H., M.K., M.O.K., L.G. F.P., J.E.M., P.F., aided in mouse studies and provided
1092 technical assistance with the experiments, M.C. aided in immunofluorescence analyses. D.S. aided
1093 in mouse studies, J.L and H.F.J, provided the RNA-Seq data of murine VSMCs. A.M and J.W.
1094 performed the mass-spectrometry analysis and analyzed the data, F.J.M. and F.F. performed
1095 statistical analysis of the ICARAS and LURIC clinical data respectively, O.D. and J.B. provided
1096 reagents and technical expertise with the experiments, and critically revised the manuscript, M.H.
1097 was involved in the analysis of human samples, T.S and N.D. provided the samples of FAST-MI
1098 clinical study and performed the statistical analysis of the data, H.S. W.M. and Z.M. provided
1099 the samples of the LURIC clinical study and measured nc-APRIL levels. G.P. provided materials,
1100 H.H. provided materials and critically revised the manuscript, Z.M. and P.S. contributed to study
1101 design, interpreted data and critically revised the manuscript, C.J.B. designed the study,
1102 interpreted data and wrote the manuscript.

1103
1104 **COMPETING INTERESTS:** DT, CJB, PS and ME are named inventors on a patent application
1105 (EP20217536.0; pending) to exploit c-APRIL and nc-APRIL for diagnostic and therapeutic
1106 purposes in cardiovascular disease that has been filed by the Medical University of Vienna
1107 (Austria) and CeMM Research Center for Molecular Medicine of the Austrian Academy of
1108 Sciences (Austria). OD is employee of Adipogen Life Sciences, which provided some reagents used
1109 in this study.

1110
1111 **Correspondence and requests for materials should be addressed to:**

1112 Dr. Dimitrios Tsiantoulas: dimitris.tsiantoulas@meduniwien.ac.at
1113 or Dr. Christoph J. Binder: christoph.binder@meduniwien.ac.at

1114

1115 **EXTENDED DATA FIGURE LEGENDS**

1116 **Extended Data Figure 1. APRIL deficiency does not alter the smooth muscle cell content,**
1117 **collagen deposition and the numbers of circulating monocytes, B and T lymphocytes in**
1118 **atherosclerotic lesions of *Ldlr*^{-/-} mice.** *Ldlr*^{-/-}*April*^{+/+} or *Ldlr*^{-/-}*April*^{-/-} mice were fed an
1119 atherogenic diet for 10 weeks. (a) Whole body weight, plasma triglyceride levels and *en face* lesion
1120 size (n= 10 *Ldlr*^{-/-}*April*^{+/+} mice and n = 12 *Ldlr*^{-/-}*April*^{-/-} mice). Representative photomicrographs
1121 of (b) DAPI, (c) α -SMA and (d) SPR2 stained lesions in the aortic origin and dot plots showing
1122 the averaged (b) acellular (n = 9 *Ldlr*^{-/-}*April*^{+/+} mice and n = 12 *Ldlr*^{-/-}*April*^{-/-} mice, P = 0.036), (c)
1123 α -SMA (n = 9 *Ldlr*^{-/-}*April*^{+/+} mice and n = 10 *Ldlr*^{-/-}*April*^{-/-} mice) and (d) collagen positive area
1124 normalized to total lesion size (n= 10 *Ldlr*^{-/-}*April*^{+/+} mice and n = 12 *Ldlr*^{-/-}*April*^{-/-} mice).
1125 Representative flow cytometry dot plots showing the (e) absolute numbers of splenic CD3⁺, CD4⁺
1126 (defined as CD3⁺ CD4⁺ CD8⁻) and CD8⁺ T cells (defined as CD3⁺ CD8⁺ CD4⁻), (f) frequencies of
1127 peritoneal B-1a (defined as B220^{low} CD11b^{int} CD5⁺), B-1b (defined as B220^{low} CD11b^{int} CD5⁻),
1128 CD23⁺ B-2 (defined as B220^{high} CD11b⁻ CD5⁻ CD23⁺) cells and (g) the frequencies of circulating
1129 Ly6C^{high}, Ly6C^{int} and Ly6C^{low} monocytes in peripheral blood. All results show mean (two-tailed
1130 unpaired Student *t* test). Scale bars: 200 μ m

1131

1132 **Extended Data Figure 2. BCMA is dispensable for atherosclerosis development.** Lethally
1133 irradiated *Ldlr*^{-/-} mice that were injected with bone marrow from *Bcma*^{+/+} (hem-*Bcma*^{+/+}; light
1134 orange) or *Bcma*^{-/-} donors (hem-*Bcma*^{-/-}; dark orange) and were fed an atherogenic diet for 10
1135 weeks. (a) Dot plot shows of *Bcma* mRNA in the spleen (n= 11 hem-*Bcma*^{+/+} and n = 13 hem-
1136 *Bcma*^{-/-} mice), (b) representative photomicrographs of H&E-stained aortic root lesions and dot plot
1137 of the average lesion size in the aortic origin expressed as μ m²/section (n = 11 hem- *Bcma*^{+/+} and
1138 n = 12 hem-*Bcma*^{-/-} mice), (c) Whole body weight, plasma triglyceride levels and *en face* lesion
1139 size (n = 11 hem-*Bcma*^{+/+} and n = 13 hem-*Bcma*^{-/-} mice). (d) Total plasma cholesterol (n = 11
1140 hem-*Bcma*^{+/+} and n = 13 hem-*Bcma*^{-/-} mice), (e) absolute numbers of FO/T2, MZ, CD21⁺CD23⁻
1141 (P = 0.028), T1 (P = 0.023), newly formed (NF) (P = 0.031) and B-1 B cells cells (n = 11 hem-
1142 *Bcma*^{+/+} and n = 13 hem-*Bcma*^{-/-} mice), (f) absolute numbers of CD3⁺, CD4⁺, CD8⁺ T cells (n =
1143 11 hem- *Bcma*^{+/+} and n = 13 hem-*Bcma*^{-/-} mice), (g) frequencies of peritoneal B-1a (P = 0.003),
1144 B-1b (P = 0.021), CD23⁺ B-2 cells (P = 0.0003) and (h) total IgM (P = 0.002), IgG1, IgG2b (P =

1145 0.002), IgG2c (P = 0.001), IgG3 (P = 0.032) and IgA plasma antibody titers (n = 11 hem- *Bcma*^{+/+}
1146 and n = 13 hem-*Bcma*^{-/-} mice). All results show mean. *P<0.05, **P<0.01, ***P<0.001, ****P
1147 <0.0001 (two-tailed Mann-Whitney *U* or two-tailed unpaired Student *t* test). Scale bar: 200 μ m.

1148

1149 **Extended Data Figure 3. APRIL is produced by mouse and human vascular smooth muscle**
1150 **cells (VSMCs).** (a) *Tnfsf13* gene expression in human tissues in the Genotype-Tissue Expression
1151 (GTEx) project¹⁴. The GTEx project was supported by the Common Fund of the Office of the
1152 Director of the National Institutes of Health, and by NCI, NHGRI, NHLBI, NIDA, NIMH, and
1153 NINDS. The data described in this manuscript were obtained from the GTEx Portal on 01/21/21
1154 and dbGaP accession number [phs000424.v8.p2](#), results show median (aorta: median = 55.05,
1155 n=432; coronary artery: median = 40.7, n = 240). (b, c) (b) Dot plot of bulk RNA-seq analysis of
1156 VSMCs from the aortic arch (AA) and descending thoracic aorta (DT) (n = 3-5 mice)
1157 (GSE117963) and (c) from mouse primary VSMCs that were stored in Trizol after isolation or had
1158 been cultured for 4-5 passages until the analysis (GSE **TO BE COMPLETED BEFORE**
1159 **PUBLICATION**). *Tnfsf13*, *Myosin-11* (*Myh11*) and *ki67* gene expression are depicted. (d) Dot
1160 plots showing the *Tnfsf13* and *IL-6* gene expression by human umbilical artery smooth muscle
1161 cells that were stimulated in quadruplicates with recombinant human TNF or native human LDL
1162 or human OxLDL (TNF stimulation is representative of three independent experiments; P = 0.003).
1163 Results show mean \pm s.e.m. **P <0.01 (1- Way ANOVA and Tukey's test).

1164

1165 **Extended Data Figure 4. APRIL binds heparan sulfate proteoglycan 2 (HSPG2).** (a)
1166 Representative photomicrographs (left) and quantification analysis (right) of HUVECs incubated
1167 with either human or mouse flag-APRIL in the presence or absence of heparin and stained with
1168 the anti-flag M2 antibody conjugated to FITC and analyzed by confocal microscopy. (b) Flow
1169 cytometry analysis of HUVECs incubated with flag-APRIL or flag-tagged bacterial alkaline
1170 phosphatase (flag-BAP) and stained with the anti-flag M2 antibody. (c) Identification of protein
1171 binding partners of APRIL in HUVEC culture by performing a pull-down assay with agarose beads
1172 coupled to the anti-flag M2 antibody followed by a mass-spectrometry analysis. (d) APRIL
1173 binding to coated HSPGs from mouse basement membrane quantified by ELISA determine in
1174 triplicates (****P <0.0001). Data shown are representative of (a, b, d) at least two independent

1175 experiments. Photomicrographs of mouse carotid artery sections incubated (e) with mouse
1176 multimeric flag-APRIL and stained with either an anti-flag antibody conjugated to PE or with an
1177 anti-mouse APRIL biotinylated antibody (2C8), (scale bar 75 μ m, data are derived from two
1178 independent experiments), (f) with mouse multimeric flag-APRIL in presence or absence of
1179 heparin and were stained with an anti-APRIL biotinylated antibody (2C8) or with an anti-HSPG2
1180 or only secondary antibody, (scale bar 75 μ m, data are derived from one experiment). (g)
1181 Quantitative Surface Plasmon Resonance (Biacore) analysis of the affinity of soluble human Fc-
1182 APRIL (total), human canonical Fc-APRIL (human Fc-c-APRIL), human non-canonical Fc-
1183 APRIL (human Fc-nc-APRIL), mouse canonical Fc-APRIL (mouse Fc-c-APRIL), mouse non-
1184 canonical Fc-APRIL (mouse Fc-nc-APRIL) and negative controls EDAR-Fc and human Fas-Fc,
1185 to biotinylated heparin coupled to streptavidin Sensor Chip A (n= 3 independent experiments). All
1186 results show mean \pm s.e.m.. ****P<0.0001, (two-tailed unpaired Student *t* test). IntDen: Integrated
1187 density.

1188

1189 **Extended Data Figure 5. Anti-APRIL antibodies 108, 2C8 and Apyr-1-1 are specific for**
1190 **mouse APRIL.** (a) Coomassie blue analyses of anti-mAPRIL mAb 108 and 2C8 under reducing
1191 conditions. (b) Isotyping of the Fc portions of anti-mAPRIL 108, Apyr-1-1 and 2C8. Purified
1192 antibodies coated on an ELISA plate were revealed with peroxidase-conjugated antibodies against
1193 different isotypes. (c) Inhibitory activity of 108 and Apyr-1-1 compared to that of TACI-Fc on
1194 human and mouse APRIL. Flag-human APRIL and two splice variants of Flag mouse APRIL (-
1195 /+Ala112) were titrated on BCMA:Fas reporter cells in the presence of a fixed, non-saturating
1196 concentration of 108, Apyr-1-1 or TACI-Fc. The data show that 108 and Apyr-1-1 inhibit both
1197 splice variants of mAPRIL at roughly stoichiometric ratios, but do not cross-react with human
1198 APRIL. (d) ELISA for 2C8 binding to mouse APRIL. Binding of 2C8 to plates coated with human
1199 Fc-mouse APRIL was evaluated with a peroxidase-coupled anti-mouse antibody. (a, b) Data are
1200 representative of two independent experiments.

1201

1202 **Extended Data Figure 6. APRIL competes the binding of LDL to proteoglycans.** (a)
1203 Representative photomicrographs (left) and quantification (right) of anti-ApoB antibody binding
1204 to murine carotid artery sections incubated with human native LDL in presence or absence of

1205 mouse multimeric flag-APRIL analyzed by both confocal and epifluorescence microscopy (w/o
1206 APRIL: n = 7 and with APRIL: n = 9, P = 0.0004). (b) A line graph showing the amount of bound
1207 human LDL (triplicates; quantified by flow cytometry) on the surface of HEK293 wild type cells
1208 in presence of different amounts of human recombinant APRIL. (c) Representative
1209 photomicrographs of ApoB-stained lesions in the aortic origin and dot plot showing the ApoB-
1210 positive area normalized to DAPI positive lesion area of *Ldlr*^{-/-}*April*^{+/+} or *Ldlr*^{-/-}*April*^{-/-} mice that
1211 were fed an atherogenic diet for 10 weeks (n = 8 *Ldlr*^{-/-}*April*^{+/+} mice and n=12 *Ldlr*^{-/-}*April*^{-/-} mice,
1212 P = 0.035). Data shown are (a) pooled from four independent experiments with seven to nine
1213 sections per group, (b) representative of three independent experiments. All results show mean ±
1214 s.e.m.. *P<0.05, ***P <0.001, (two-tailed unpaired Student *t* test), scale bars: (a) 20 μm and (c)
1215 200 μm.

1216

1217 **Extended Data Figure 7. Treatment with the blocking anti-APRIL antibody Apyr1-1 does**
1218 **not alter B cell responses and plasma lipid levels in *ApoE*^{-/-} mice.** *ApoE*^{-/-} mice were treated
1219 biweekly for 10 weeks with a mixture of either mouse anti-APRIL antibody (Apyr-1-1) and Ctrl-
1220 Ig (α-APRIL group), or TACI-Ig and isotype IgG2b (TACI-Ig group), or isotype IgG2b and Ctrl-
1221 Ig (Ctrl group) and were fed an atherogenic diet for the last 8 weeks of the study. Dot plots showing
1222 the numbers of (a) total splenic B cells, (b) follicular (FO) B cells, (c) marginal zone (MZ) B cells,
1223 frequencies of (d) peritoneal B-1a, (e) peritoneal B-1b and (f) total IgM antibody levels in plasma.
1224 (g) Wild-type mice were injected intraperitoneally with either 1μg of mouse multimeric flag-
1225 APRIL or a mixture of 1μg flag-APRIL and 10μg anti-mouse APRIL antibody (Apyr-1-1). The
1226 amount of flag-APRIL in plasma was measured by ELISA one, three and six hours after the
1227 injection (n = 4 mice APRIL-flag, n = 5 mice APRIL-flag+ α-APRIL (Apyr1-1)). (h) Whole body
1228 weight, plasma triglyceride and cholesterol levels. (a, b, c, d, e, f, h) All results show mean ±
1229 s.e.m. of n = 10 *ApoE*^{-/-}; Ctrl, n = 12 *ApoE*^{-/-}; TACI-Ig, n = 10 *ApoE*^{-/-}; α-APRIL). ***P <0.001,
1230 ****P <0.0001 (1- Way ANOVA and Newman-Keuls test).

1231

1232 **Extended Data Figure 8. (a-h) Epitope mapping of anti-human APRIL antibodies.** (a) The
1233 epitopes recognized by Apyrily1, 2, 3, 5 and 10 were mapped by Western Blot of truncated APRIL
1234 proteins. (b, c, d) Apyrily5 and Apyrily1 or 2 recognize distinct epitopes, (e, f) while Apyrily3 and 10

1235 recognize epitopes distinct from those of Aprily1, Aprily2 and Aprily5. **(g)** Expression of all
1236 constructs was validated by Western Blot with anti-Fc antibody. **(h, i)** Human serum was depleted
1237 of APRIL using the anti-human APRIL antibodies: Aprily1, Aprily2, Aprily3, Aprily5, Aprily6,
1238 Aprily8, Aprily9, Aprily10, Mahya-1, 110.6 or the biological atacept (TACI-Ig: a recombinant
1239 fusion protein of the receptor TACI and the Fc region of Ig, that binds to APRIL) or the negative
1240 control EctoD1 and then analyzed with **(h)** a c-APRIL specific (ELISA 1) or **(i)** a nc-APRIL
1241 specific ELISA (ELISA 2) Data are derived from one experiment in this format. **(j-n) Native**
1242 **canonical and non-canonical APRIL differ in size.** **(j)** Flag-human APRIL (from c-APRIL
1243 ELISA 1 standards) was depleted on TACI-Fc (or TNFR2-Fc as control) and/or on Aprily2 (or
1244 mIgG1 as control). APRIL was then detected by c-APRIL specific (top) or nc-APRIL specific
1245 (bottom) ELISA. **(k, l)** Flag-human APRIL (from Adipogen ELISA standards) was depleted on
1246 immobilized TACI-Fc or on Aprily2, and the flow through was then size-fractionated by size
1247 exclusion chromatography (SEC) and detected in fractions by **(k)** c-APRIL specific (ELISA 1) or
1248 **(l)** nc-APRIL specific (ELISA 2) ELISA. TACI-Fc and Aprily2 beads used for depletion were then
1249 acid-eluted. **(m, n)** The neutralized eluate was size-fractionated, and APRIL in fractions were
1250 detected with **(m)** c-APRIL specific or **(n)** nc-APRIL specific ELISA. These results indicate that
1251 Flag-c-APRIL has the size of a 3-mer, while nc-APRIL is much larger. **(o, p) Canonical and non-**
1252 **canonical APRIL are produced by the same *Tnfsf13* gene locus.** The *Tnfsf13* gene (which
1253 encodes APRIL) was inactivated in human macrophage cell line U937 by CRISPR/Cas9
1254 technology. As a control the *Tnfsf13b* gene (which encodes BAFF) was also deleted. APRIL in
1255 supernatants was measured with **(o)** a c-APRIL specific and **(p)** a nc-APRIL specific ELISA. (105,
1256 110, 301 and 302 depict different clones).

1257

1258 **Extended Data Figure 9. LC-MS-based Parallel Reaction Monitoring (PRM) analysis of**
1259 **tryptic digest of purified human canonical or non-canonical Fc-APRIL.** Raw data was
1260 analyzed using Skyline software and extracted product ion chromatograms (XICs) are shown
1261 either in form of peaks (upper panel) or total sum of integrated product ion areas (lower panel) for
1262 the three selected peptides **(a)** EEQYNSTYR (Fc part), **(b)** LNLSPHGTFLGFVK (tryptic C-
1263 terminus APRIL) and **(c)** LNLSPHGTFLGFVKL (miscleaved tryptic C-terminus APRIL). MS2
1264 fragment ion spectra for the selected peptide precursor ions are illustrated in the lower right panel.
1265 While the peptide shown in (a) is representative for comparable injection amounts of canonical

1266 versus non-canonical Fc-APRIL, the C-terminal miscleaved full tryptic peptide shown in (c) is
1267 undetectable in non-canonical APRIL. Relative abundances are given in arbitrary units. Right
1268 panel illustrates the FASTA sequence of Fc-APRIL with selected tryptic peptide sequences
1269 highlighted in blue or red. Note the different scales in panels (b) (10^9) and (c) (10^6). (d) Structure
1270 of human c-APRIL highlighting the importance of the C-terminus for the folding of the different
1271 forms (canonical and non-canonical) of APRIL. The representation based on protein data
1272 bank accession number 1XU1 highlights the last two C-terminal amino acids (Lys232,
1273 Leu233). The N-terminal amino acid of the TNF homology domain (His98), and
1274 Asp142 are also shown. All of these residues are conserved in mouse APRIL and human
1275 APRIL, although the sequence surrounding Asp142 is different in mouse and human.
1276 The C-terminal carboxylic group of Leu233 is very close to His98 of the same monomer
1277 (3.6 Å, 4.1 Å and 3.4 Å in the three monomers) and also very close to His98 of the
1278 neighbouring monomer (4.3 Å, 3.8 Å and 3.8 Å). Thus, H98 and the carboxylic group
1279 or Leu233 seem to form a ring of 6 salt bridges at the top surface of APRIL. In addition,
1280 Lys232 contacts Asp142 (4.3 Å, 4.3 Å and 5.7 Å in the three mouse APRIL monomers,
1281 and is at only 3.2 Å of Asp142 in human APRIL (pdb accession number 4ZCH).

1282

1283 **Extended Data Table 1. Human clinical studies.** (a) Univariate and multivariate Cox
1284 Regression analyses of the ICARAS study (nc-APRIL). 1st Tertile includes patients with nc-
1285 APRIL levels lower than 4.22 ng/ml, 2nd tertile patients with nc-APRIL levels between 4.23 to
1286 6.47 ng/ml, the 3rd tertile patients with nc-APRIL levels above 6.47 ng/ml. Adjusted for age, sex,
1287 body mass index, smoking, hypertension, low-density lipoprotein cholesterol levels, triglyceride
1288 levels, statin treatment, glycohemoglobin A1 level, diabetes mellitus, history of myocardial
1289 infarction, history of peripheral artery disease, history of stroke, and serum creatinine, intercellular
1290 adhesion molecule-1, vascular cell adhesion molecule-1, and high-sensitivity C-reactive protein.
1291 The third tertile serves as the reference category, (n=785). (b) Univariate and multivariate Cox
1292 Regression analyses of the ICARAS study (c-APRIL). 1st Tertile includes patients with APRIL
1293 levels lower than 1.67 ng/ml, 2nd tertile patients with APRIL levels between 1.67 to 2.54 ng/ml,
1294 the 3rd tertile patients with APRIL levels above 2.54 ng/ml. Adjusted for age, sex, body mass index,

1295 smoking, hypertension, low-density lipoprotein cholesterol levels, triglyceride levels, statin
1296 treatment, glycohemoglobin A1 level, diabetes mellitus, history of myocardial infarction, history
1297 of peripheral artery disease, history of stroke, and serum creatinine, intercellular adhesion
1298 molecule-1, vascular cell adhesion molecule-1, and high-sensitivity C-reactive protein. The third
1299 tertile serves as the reference category (n=730). (c) Multivariate Cox Regression analyses for
1300 cardiovascular mortality in the LURIC study (nc-APRIL). Adjusted for age (years), sex
1301 (male/female), C-reactive protein (mg/dL), triglycerides (mg/dL), total cholesterol levels (mg/dL),
1302 history of myocardial infarction (binary), history of stroke (binary), peripheral arterial disease
1303 (binary), body mass index (kg/m²), hypertension (binary), diabetes mellitus (binary), serum
1304 creatinine (mg/dL), hemoglobin 1AC (percent) (n=1,514). (d) Multivariate Cox Regression
1305 analyses French registry of Acute ST elevation or non-ST-elevation Myocardial Infarction clinical
1306 study (FAST-MI). Circulating levels of nc-APRIL in patients at the admission for acute
1307 myocardial infarction are associated with cardiovascular outcomes at follow-up. The probability
1308 of death during 2 years of follow-up as a function of baseline circulating plasma APRIL levels
1309 (n=974). Results are expressed as hazard ratios (HR) with 95% confidence intervals (CIs).

1310 **REFERENCES (altogether as ENDNOTE library):**

- 1311 1. World Health Organization. Global status report on noncommunicable diseases 2014. xvii,
1312 280 pages (World Health Organization,, Geneva, Switzerland, 2014).
- 1313 2. World Health Organization, Noncommunicable diseases country profiles 2018, ISBN: 978
1314 92 4 151462 0. (2018).
- 1315 3. Gistera, A. & Hansson, G.K. The immunology of atherosclerosis. *Nat Rev Nephrol* **13**,
1316 368-380 (2017).
- 1317 4. Ingold, K., *et al.* Identification of proteoglycans as the APRIL-specific binding partners. *J*
1318 *Exp Med* **201**, 1375-1383 (2005).
- 1319 5. Vincent, F.B., Morand, E.F., Schneider, P. & Mackay, F. The BAFF/APRIL system in SLE
1320 pathogenesis. *Nat Rev Rheumatol* **10**, 365-373 (2014).
- 1321 6. Castigli, E., *et al.* Impaired IgA class switching in APRIL-deficient mice. *Proc Natl Acad*
1322 *Sci U S A* **101**, 3903-3908 (2004).
- 1323 7. Huard, B., *et al.* APRIL secreted by neutrophils binds to heparan sulfate proteoglycans to
1324 create plasma cell niches in human mucosa. *J Clin Invest* **118**, 2887-2895 (2008).
- 1325 8. McCarron, M.J., Park, P.W. & Fooksman, D.R. CD138 mediates selection of mature
1326 plasma cells by regulating their survival. *Blood* **129**, 2749-2759 (2017).
- 1327 9. Hymowitz, S.G., *et al.* Structures of APRIL-receptor complexes: like BCMA, TACI
1328 employs only a single cysteine-rich domain for high affinity ligand binding. *J Biol Chem*
1329 **280**, 7218-7227 (2005).
- 1330 10. Sandberg, W.J., *et al.* The tumour necrosis factor superfamily ligand APRIL (TNFSF13)
1331 is released upon platelet activation and expressed in atherosclerosis. *Thromb Haemost* **102**,
1332 704-710 (2009).

- 1333 11. Mackay, F. & Schneider, P. Cracking the BAFF code. *Nat Rev Immunol* **9**, 491-502 (2009).
- 1334 12. Tsiantoulas, D., *et al.* B Cell-Activating Factor Neutralization Aggravates Atherosclerosis.
- 1335 *Circulation* **138**, 2263-2273 (2018).
- 1336 13. Patel, D.R., *et al.* Engineering an APRIL-specific B cell maturation antigen. *J Biol Chem*
- 1337 **279**, 16727-16735 (2004).
- 1338 14. Consortium, G.T., *et al.* Genetic effects on gene expression across human tissues. *Nature*
- 1339 **550**, 204-213 (2017).
- 1340 15. Hellings, W.E., Moll, F.L., de Kleijn, D.P. & Pasterkamp, G. 10-years experience with the
- 1341 Athero-Express study. *Cardiovasc Diagn Ther* **2**, 63-73 (2012).
- 1342 16. Lord, M.S., *et al.* The multifaceted roles of perlecan in fibrosis. *Matrix Biol* **68-69**, 150-
- 1343 166 (2018).
- 1344 17. Vikramadithyan, R.K., *et al.* Atherosclerosis in perlecan heterozygous mice. *J Lipid Res*
- 1345 **45**, 1806-1812 (2004).
- 1346 18. Tran-Lundmark, K., *et al.* Heparan sulfate in perlecan promotes mouse atherosclerosis:
- 1347 roles in lipid permeability, lipid retention, and smooth muscle cell proliferation. *Circ Res*
- 1348 **103**, 43-52 (2008).
- 1349 19. Skalen, K., *et al.* Subendothelial retention of atherogenic lipoproteins in early
- 1350 atherosclerosis. *Nature* **417**, 750-754 (2002).
- 1351 20. Sarrazin, S., Lamanna, W.C. & Esko, J.D. Heparan sulfate proteoglycans. *Cold Spring*
- 1352 *Harb Perspect Biol* **3**(2011).
- 1353 21. Parish, C.R. The role of heparan sulphate in inflammation. *Nat Rev Immunol* **6**, 633-643
- 1354 (2006).
- 1355 22. Bernelot Moens, S.J., *et al.* Impact of the B Cell Growth Factor APRIL on the Qualitative
- 1356 and Immunological Characteristics of Atherosclerotic Plaques. *PLoS One* **11**, e0164690
- 1357 (2016).
- 1358 23. Haselmayer, P., Vigolo, M., Nys, J., Schneider, P. & Hess, H. A mouse model of systemic
- 1359 lupus erythematosus responds better to soluble TACI than to soluble BAFFR, correlating
- 1360 with depletion of plasma cells. *Eur J Immunol* **47**, 1075-1085 (2017).
- 1361 24. Tsiantoulas, D., *et al.* BAFF Neutralization Aggravates Atherosclerosis. *Circulation*
- 1362 (2018).
- 1363 25. Kyaw, T., *et al.* B1a B lymphocytes are atheroprotective by secreting natural IgM that
- 1364 increases IgM deposits and reduces necrotic cores in atherosclerotic lesions. *Circ Res* **109**,
- 1365 830-840 (2011).
- 1366 26. Gruber, S., *et al.* Sialic Acid-Binding Immunoglobulin-like Lectin G Promotes
- 1367 Atherosclerosis and Liver Inflammation by Suppressing the Protective Functions of B-1
- 1368 Cells. *Cell Rep* (2016).
- 1369 27. Rosenfeld, S.M., *et al.* B-1b Cells Secrete Atheroprotective IgM and Attenuate
- 1370 Atherosclerosis. *Circ Res* **117**, e28-39 (2015).
- 1371 28. Lewis, M.J., *et al.* Immunoglobulin M is required for protection against atherosclerosis in
- 1372 low-density lipoprotein receptor-deficient mice. *Circulation* **120**, 417-426 (2009).
- 1373 29. Tsiantoulas, D., *et al.* Increased Plasma IgE Accelerate Atherosclerosis in Secreted IgM
- 1374 Deficiency. *Circ Res* **120**, 78-84 (2017).
- 1375 30. Dishman, A.F., *et al.* Evolution of fold switching in a metamorphic protein. *Science* **371**,
- 1376 86-90 (2021).
- 1377 31. Schillinger, M., *et al.* Inflammation and Carotid Artery--Risk for Atherosclerosis Study
- 1378 (ICARAS). *Circulation* **111**, 2203-2209 (2005).

- 1379 32. Winkelmann, B.R., *et al.* Rationale and design of the LURIC study--a resource for
1380 functional genomics, pharmacogenomics and long-term prognosis of cardiovascular
1381 disease. *Pharmacogenomics* **2**, S1-73 (2001).
- 1382 33. Puymirat, E., *et al.* Acute Myocardial Infarction: Changes in Patient Characteristics,
1383 Management, and 6-Month Outcomes Over a Period of 20 Years in the FAST-MI Program
1384 (French Registry of Acute ST-Elevation or Non-ST-Elevation Myocardial Infarction) 1995
1385 to 2015. *Circulation* **136**, 1908-1919 (2017).
- 1386 34. Kowalczyk-Quintas, C., *et al.* Generation and characterization of function-blocking anti-
1387 ectodysplasin A (EDA) monoclonal antibodies that induce ectodermal dysplasia. *J Biol*
1388 *Chem* **289**, 4273-4285 (2014).
- 1389 35. Tsiantoulas, D., *et al.* Increased Plasma IgE Accelerate Atherosclerosis in Secreted IgM
1390 Deficiency. *Circ Res* (2016).
- 1391 36. Chou, M.Y., *et al.* Oxidation-specific epitopes are dominant targets of innate natural
1392 antibodies in mice and humans. *J Clin Invest* **119**, 1335-1349 (2009).
- 1393 37. Kijani, S., Vazquez, A.M., Levin, M., Boren, J. & Fogelstrand, P. Intimal hyperplasia
1394 induced by vascular intervention causes lipoprotein retention and accelerated
1395 atherosclerosis. *Physiol Rep* **5**(2017).
- 1396 38. Tom, R., Bisson, L. & Durocher, Y. Transfection of HEK293-EBNA1 Cells in Suspension
1397 with Linear PEI for Production of Recombinant Proteins. *CSH Protoc* **2008**, pdb prot4977
1398 (2008).
- 1399 39. Schindelin, J., *et al.* Fiji: an open-source platform for biological-image analysis. *Nat*
1400 *Methods* **9**, 676-682 (2012).
- 1401 40. Bossen, C., *et al.* TACI, unlike BAFF-R, is solely activated by oligomeric BAFF and
1402 APRIL to support survival of activated B cells and plasmablasts. *Blood* **111**, 1004-1012
1403 (2008).
- 1404 41. Kowalczyk-Quintas, C., *et al.* Inhibition of Membrane-Bound BAFF by the Anti-BAFF
1405 Antibody Belimumab. *Front Immunol* **9**, 2698 (2018).
- 1406 42. Schneider, P., Willen, L. & Smulski, C.R. Tools and techniques to study ligand-receptor
1407 interactions and receptor activation by TNF superfamily members. *Methods in enzymology*
1408 **545**, 103-125 (2014).
- 1409 43. Manza, L.L., Stamer, S.L., Ham, A.-J.L., Codreanu, S.G. & Liebler, D.C. Sample
1410 preparation and digestion for proteomic analyses using spin filters. *Proteomics* **5**, 1742-
1411 1745 (2005).
- 1412 44. Wisniewski, J.R., Zougman, A., Nagaraj, N. & Mann, M. Universal sample preparation
1413 method for proteome analysis. *Nat Meth* **6**, 359-362 (2009).
- 1414 45. Rappsilber, J., Ishihama, Y. & Mann, M. Stop and Go Extraction Tips for Matrix-Assisted
1415 Laser Desorption/Ionization, Nanoelectrospray, and LC/MS Sample Pretreatment in
1416 Proteomics. *Anal Chem* **75**, 663-670 (2003).
- 1417 46. Olsen, J.V., *et al.* Parts per Million Mass Accuracy on an Orbitrap Mass Spectrometer via
1418 Lock Mass Injection into a C-trap. *Mol Cell Proteomics* **4**, 2010-2021 (2005).
- 1419 47. Mayer, F.J., *et al.* Combined Effects of Inflammatory Status and Carotid Atherosclerosis:
1420 A 12-Year Follow-Up Study. *Stroke* **47**, 2952-2958 (2016).

1421

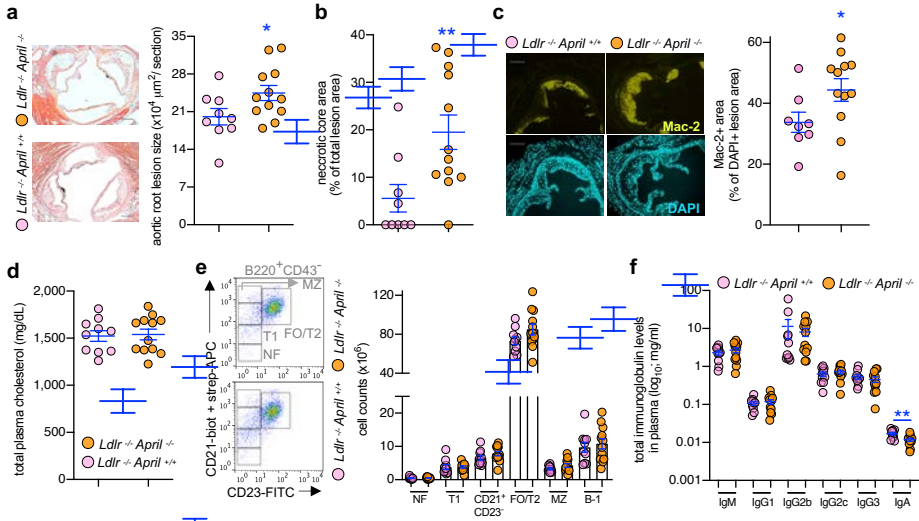


Figure 1

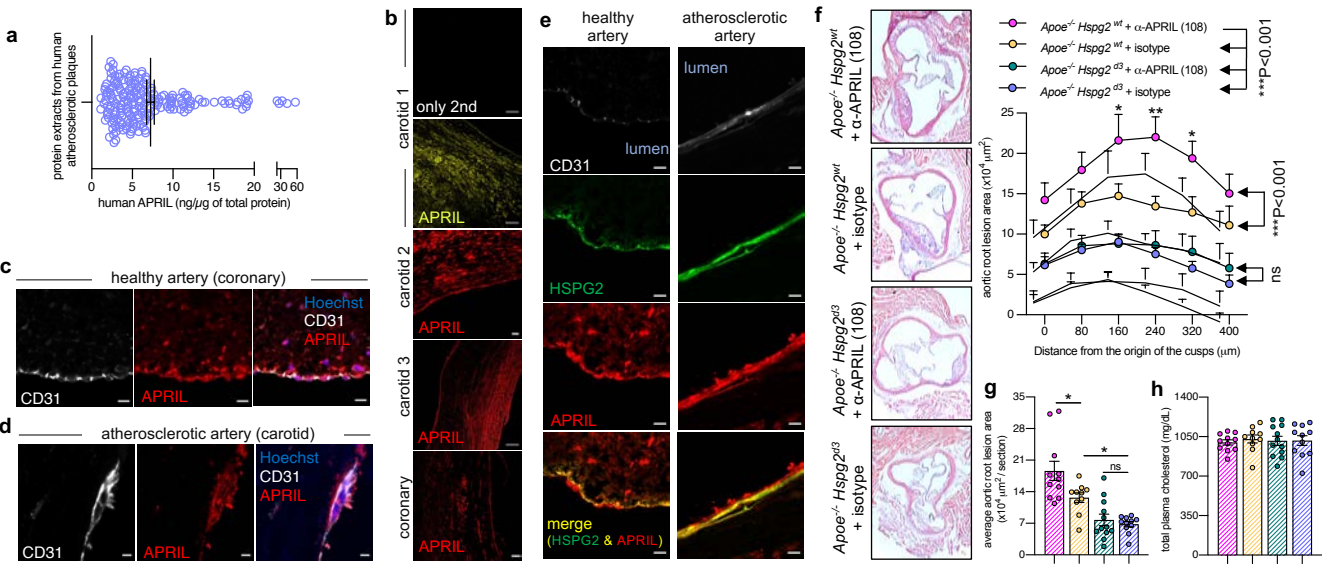


Figure 2

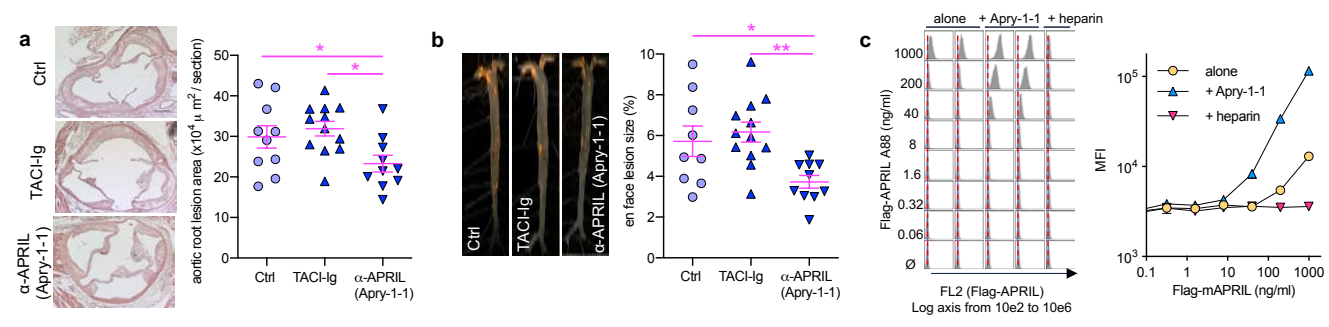


Figure 3

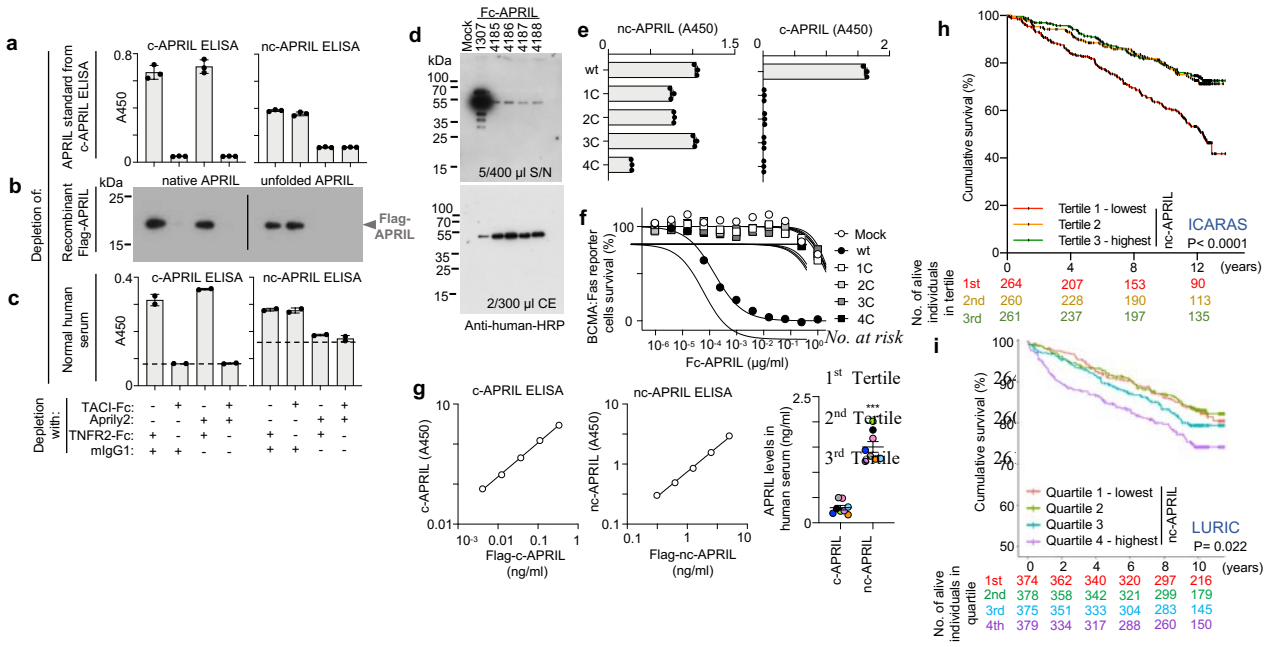
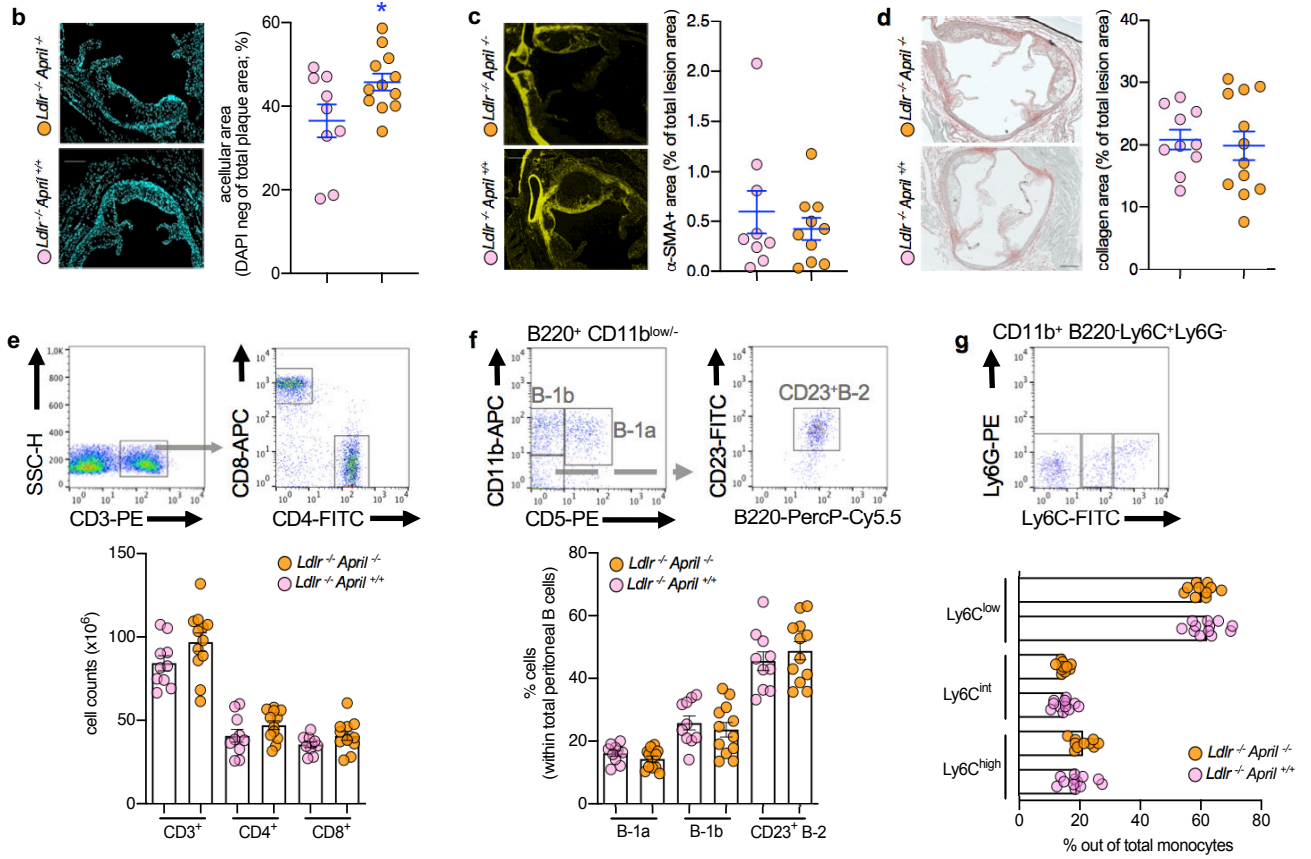


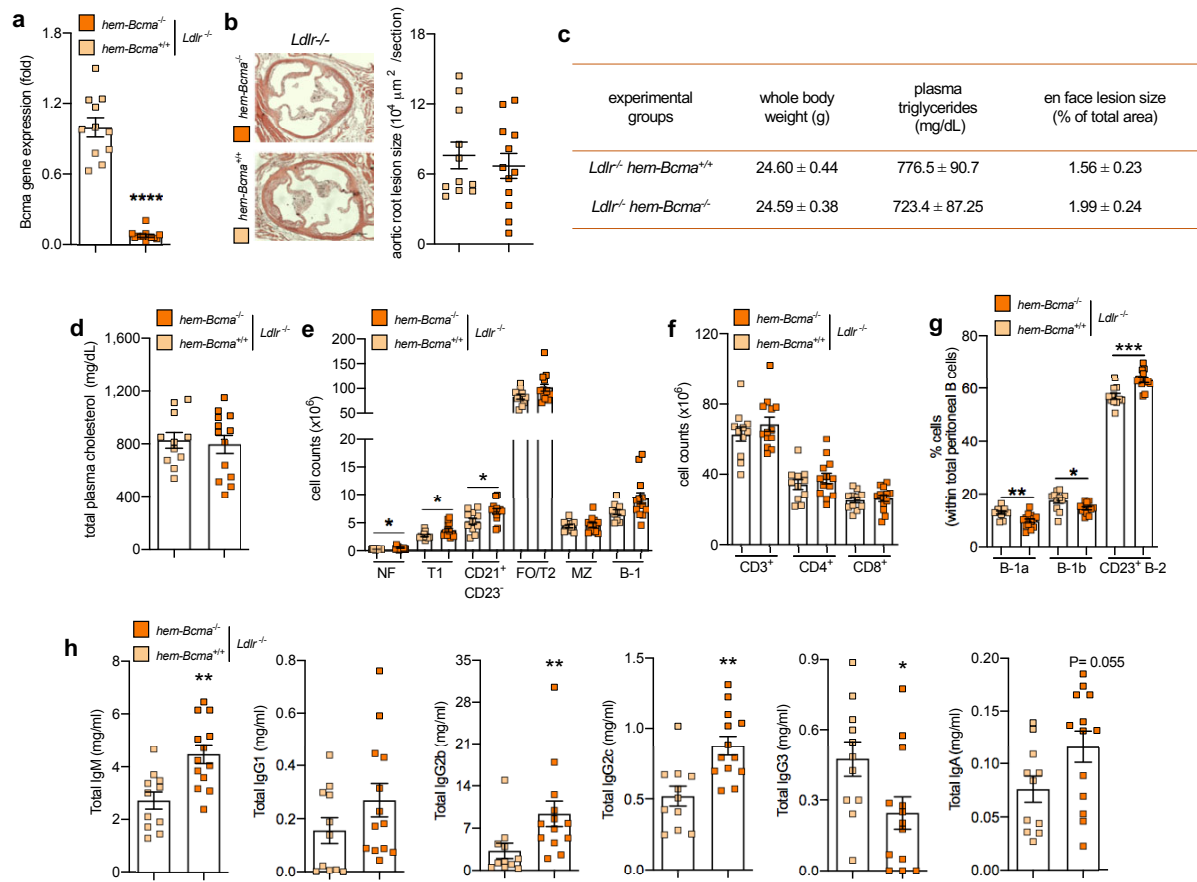
Figure 4

a

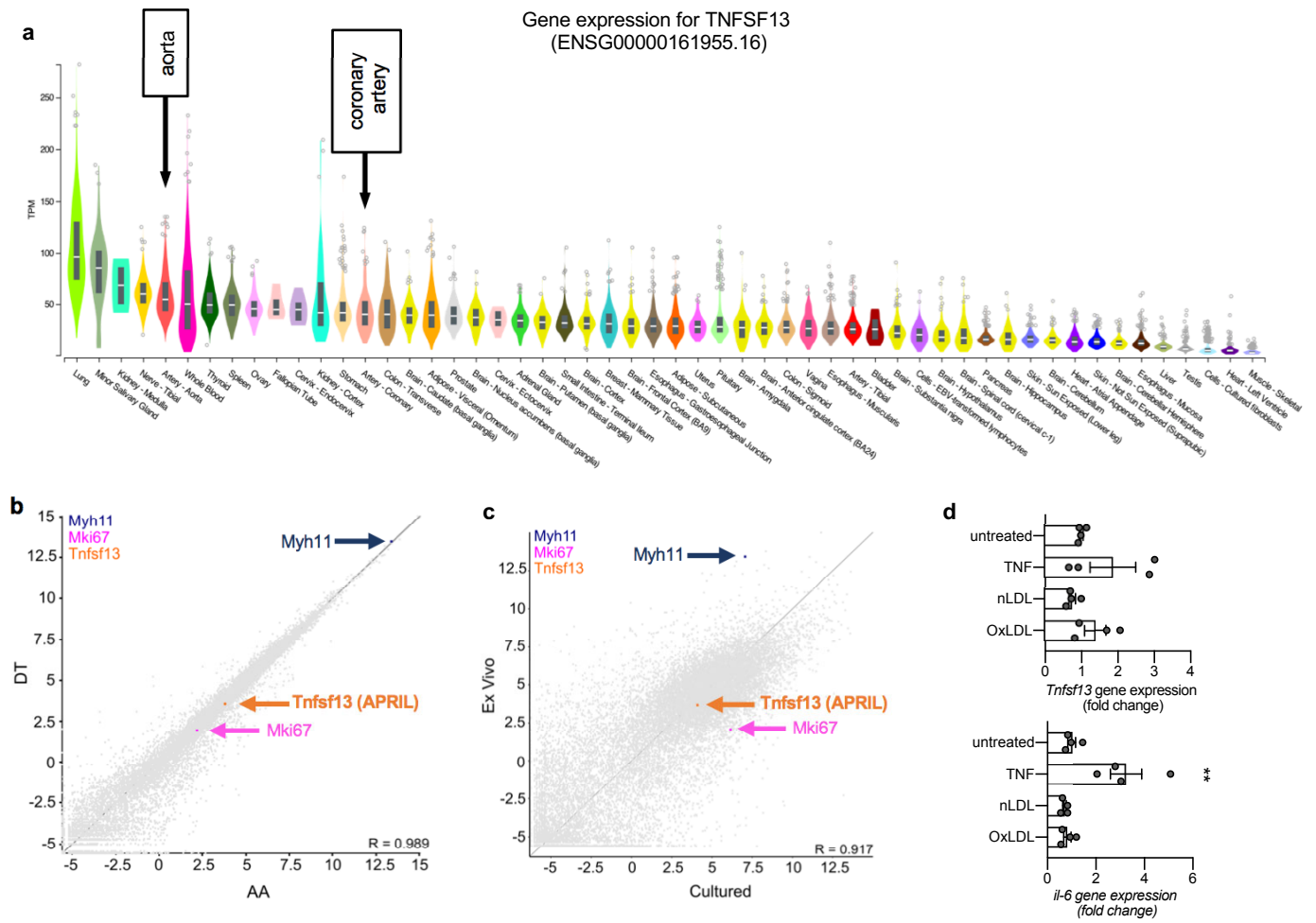
experimental groups	whole body weight (g)	plasma triglycerides (mg/dL)	en face lesion size (% of total area)
<i>Ldlr</i> ^{-/-} <i>April</i> ^{+/-}	22.98 ± 0.74	665.0 ± 53.61	1.89 ± 0.19
<i>Ldlr</i> ^{-/-} <i>April</i> ^{-/-}	23.28 ± 0.40	596.9 ± 43.06	1.67 ± 0.20



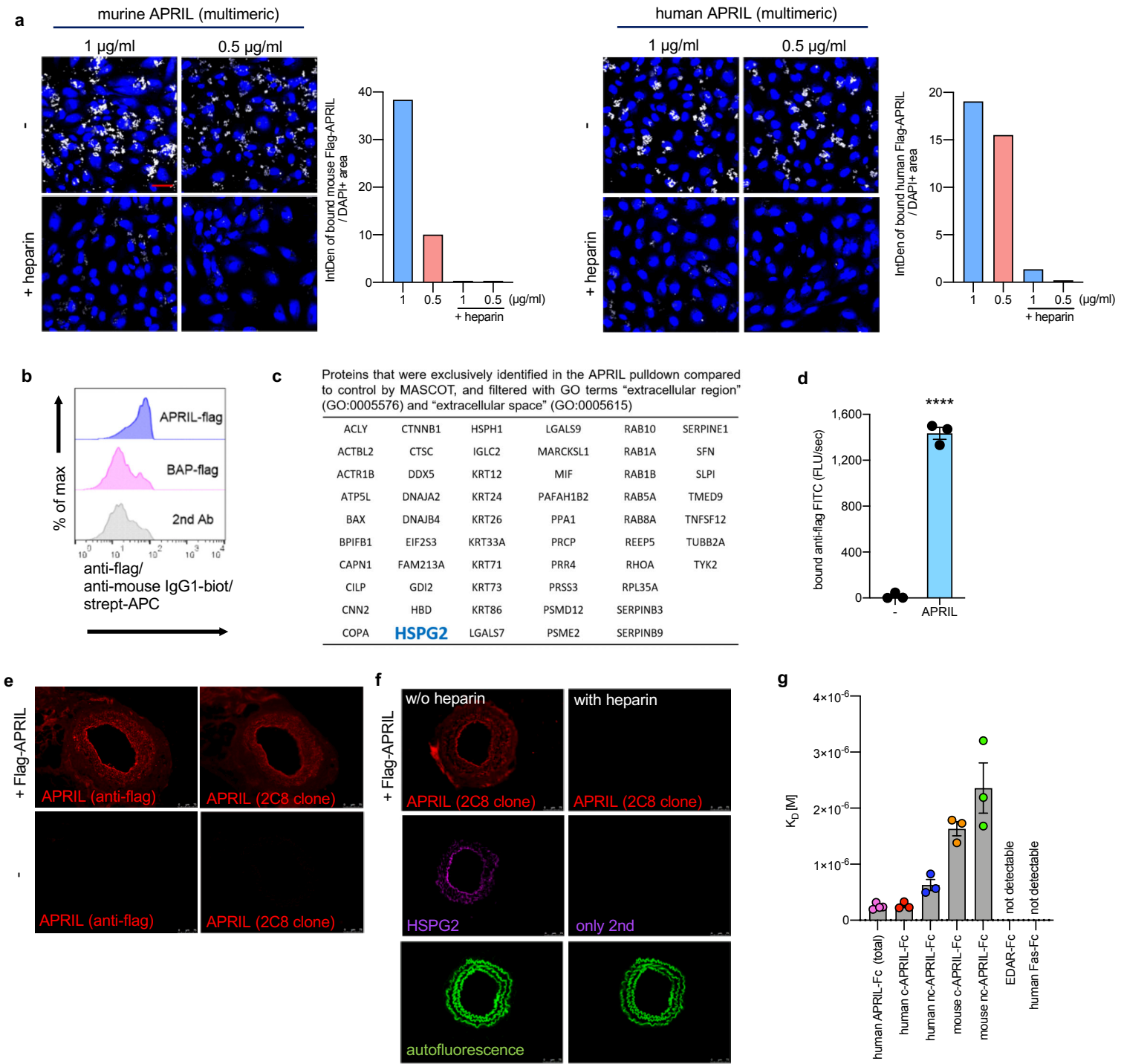
Extended Data Figure 1



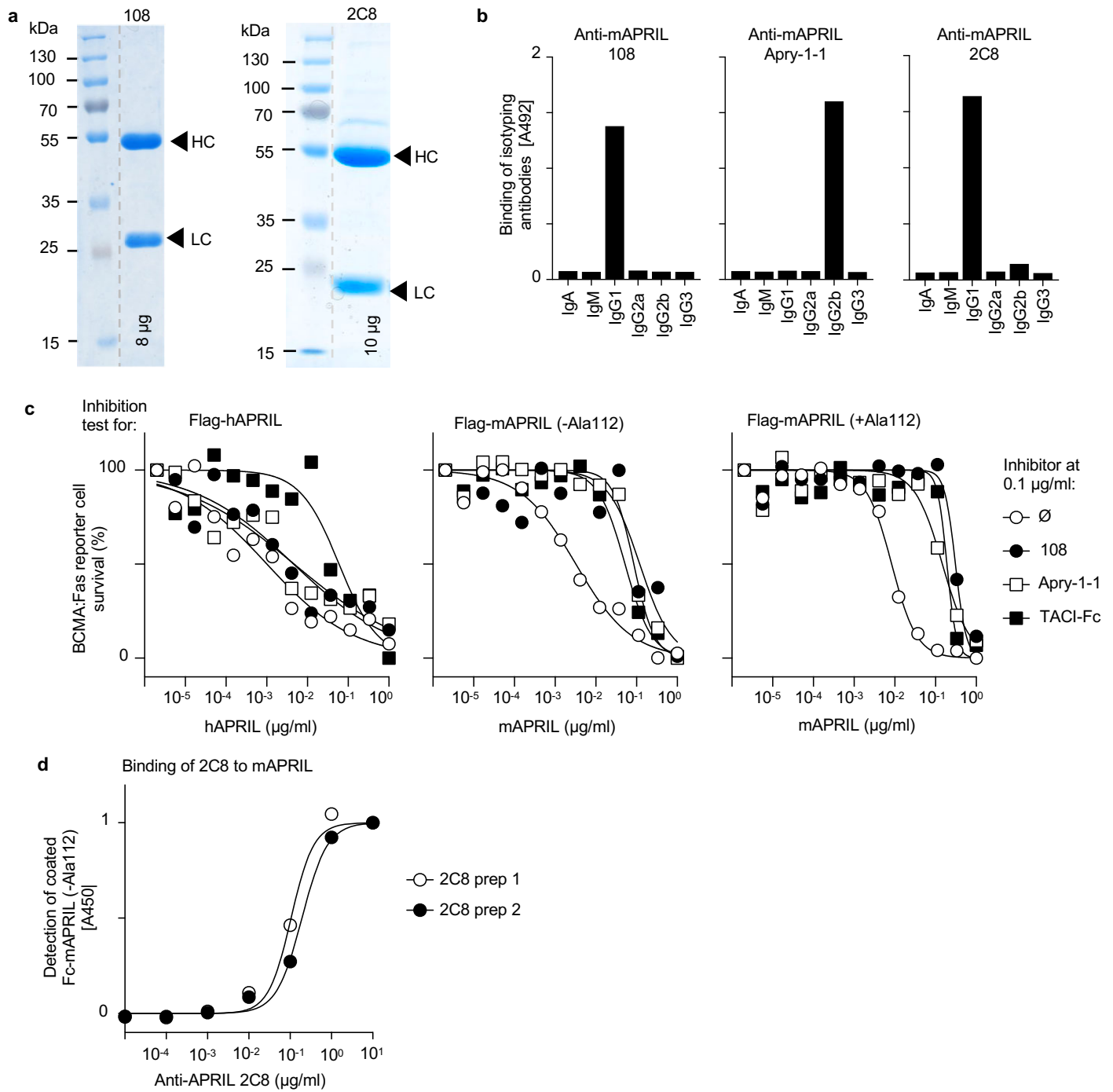
Extended Data Figure 2



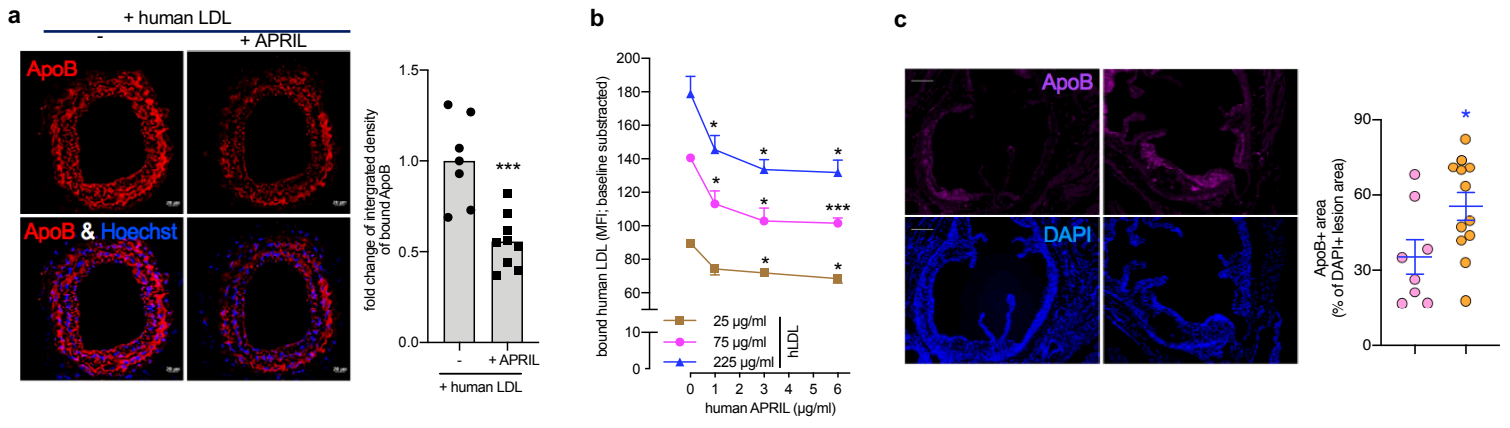
Extended Data Figure 3



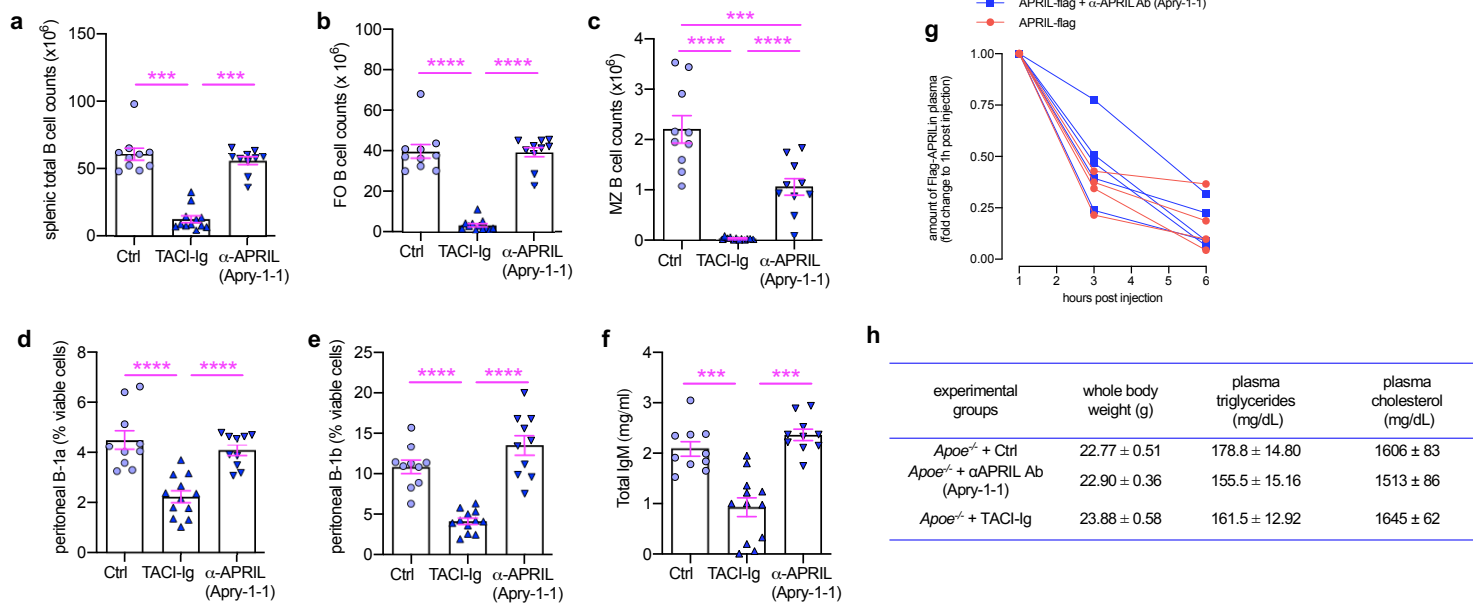
Extended Data Figure 4



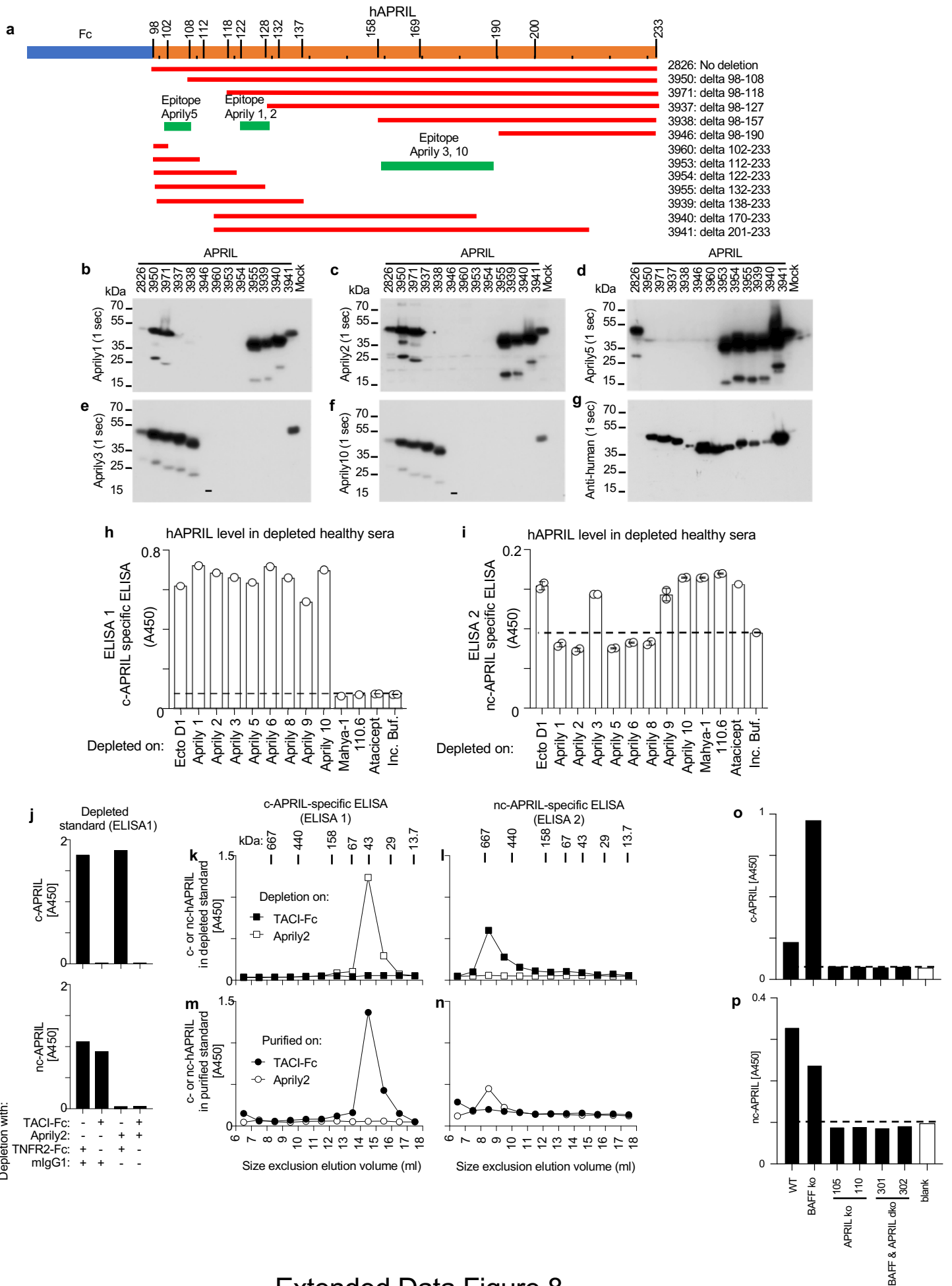
Extended Data Figure 5



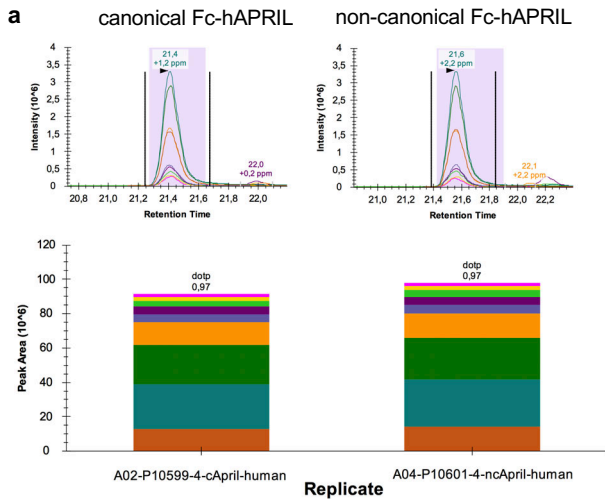
Extended Data Figure 6



Extended Data Figure 7

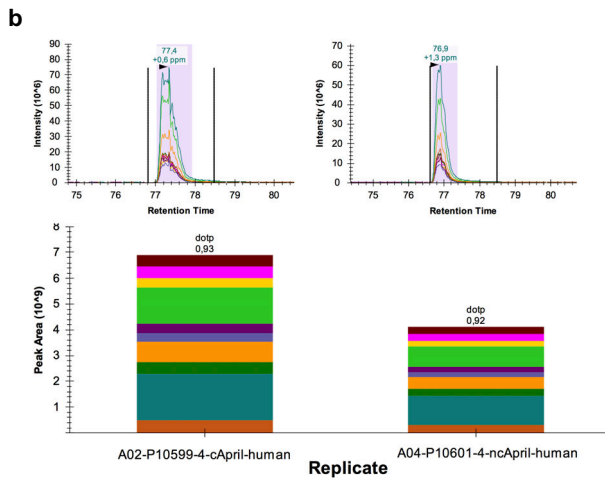
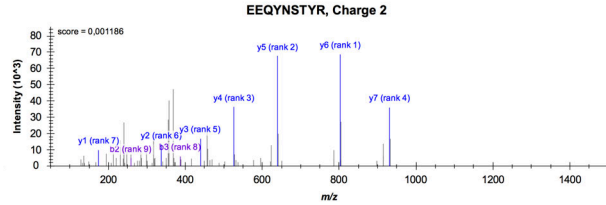


Extended Data Figure 8

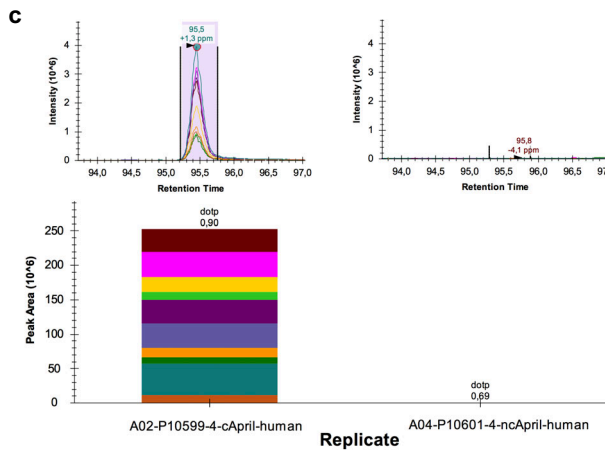
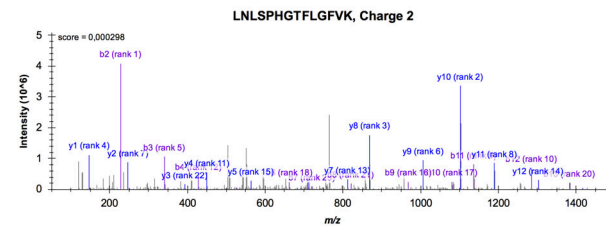


FASTA sequence of human Fc-hAPRIL

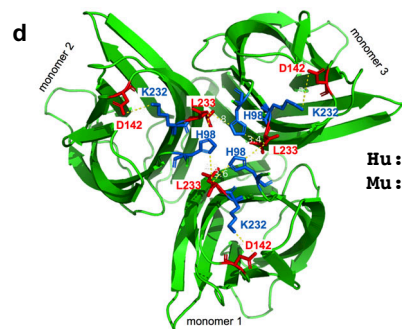
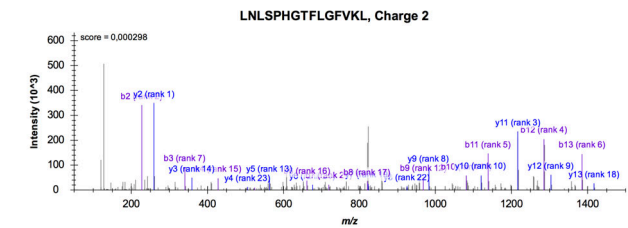
LDKTHTCPPCPAPELLGGPSVFLFPPKPKDLMISRTEVTCVVVDVSHEDP
 EVKFNWYVDGVEVHNAKTKPRE**EEQYNSTYR**VVSVLTVLHQDWLNGKEYKCKV
 SNKALPAPIEKTISKAKGQPREPQVYTLPPSRDELTKNQVSLTCLVKGFYPS
 DIAVEWESNGQPENNYKTTPPVLDSDGSFFLYSKLTVDKSRWQQGNVFCSSV
 MHEALHNHYTQKSLSLSPGKRSPQPKPQPKPEPEGSLEVLVFGPGSLQHS
 VLHLVPIINATSKDDSDVTEVMWQPALRRRGRGLQAQGYGVRIQDAGVYLLYSQ
 VLFQDVFTFMGQVVSREGQGRQETLFR CIRMPSPHPDRAYNSCYSAGVFHLH
 QGDILSVIIPRARKLNLSPHGTFGLGFVKL



LDKTHTCPPCPAPELLGGPSVFLFPPKPKDLMISRTEVTCVVVDVSHEDP
 EVKFNWYVDGVEVHNAKTKPRE**EQYNSTYR**VVSVLTVLHQDWLNGKEYKCKV
 SNKALPAPIEKTISKAKGQPREPQVYTLPPSRDELTKNQVSLTCLVKGFYPS
 DIAVEWESNGQPENNYKTTPPVLDSDGSFFLYSKLTVDKSRWQQGNVFCSSV
 MHEALHNHYTQKSLSLSPGKRSPQPKPQPKPEPEGSLEVLVFGPGSLQHS
 VLHLVPIINATSKDDSDVTEVMWQPALRRRGRGLQAQGYGVRIQDAGVYLLYSQ
 VLFQDVFTFMGQVVSREGQGRQETLFR CIRMPSPHPDRAYNSCYSAGVFHLH
 QGDILSVIIPRARK**LNLSPHGTFGLGFVKL**



LDKTHTCPPCPAPELLGGPSVFLFPPKPKDLMISRTEVTCVVVDVSHEDP
 EVKFNWYVDGVEVHNAKTKPRE**EQYNSTYR**VVSVLTVLHQDWLNGKEYKCKV
 SNKALPAPIEKTISKAKGQPREPQVYTLPPSRDELTKNQVSLTCLVKGFYPS
 DIAVEWESNGQPENNYKTTPPVLDSDGSFFLYSKLTVDKSRWQQGNVFCSSV
 MHEALHNHYTQKSLSLSPGKRSPQPKPQPKPEPEGSLEVLVFGPGSLQHS
 VLHLVPIINATSKDDSDVTEVMWQPALRRRGRGLQAQGYGVRIQDAGVYLLYSQ
 VLFQDVFTFMGQVVSREGQGRQETLFR CIRMPSPHPDRAYNSCYSAGVFHLH
 QGDILSVIIPRARK**LNLSPHGTFGLGFVKL**



Hu: QHSV[...]VRIQDAG[...]GFVKL
 Mu: KHSV[...]VRVDTG[...]GFVKL
 H98 D142 K232L233

a **ICARAS (nc-APRIL)**

Variable	Univariate			Multivariate		
	Hazard ratio	CI	P-value	Hazard ratio	CI	P-value
All-Cause Mortality						
3 rd Tertile* (>6.47 ng/ml)	-	-	-	-	-	-
2 nd Tertile (4.23-6.47 ng/ml)	1.17	0.90-1.52	0.25	1.31	0.97-1.77	0.07
1 st Tertile (<4.22 ng/ml)	1.99	1.56-2.54	<0.01	1.95	1.48-2.56	<0.01
Cardiovascular Mortality						
3 rd Tertile* (>6.47 ng/ml)	-	-	-	-	-	-
2 nd Tertile (4.23-6.47 ng/ml)	1.08	0.76-1.52	0.68	1.28	0.86-1.91	0.22
1 st Tertile (<4.22 ng/ml)	2.27	1.67-3.07	<0.01	2.20	1.56-3.12	<0.01

*Reference Category

b **ICARAS (c-APRIL)**

Variable	Univariate		Multivariate	
	Hazard ratio	P-value	Hazard ratio	P-value
All-Cause Mortality				
3 rd Tertile* (>2.54 ng/ml)	-	-	-	-
2 nd Tertile (1.67-2.54 ng/ml)	1.03	0.82	0.94	0.67
1 st Tertile (<1.67 ng/ml)	1.07	0.63	1.13	0.41
Cardiovascular Mortality				
3 rd Tertile* (>2.54 ng/ml)	-	-	-	-
2 nd Tertile (1.67-2.54 ng/ml)	0.89	0.38	0.78	0.21
1 st Tertile (<1.67 ng/ml)	1.0	0.89	1.19	0.35

*Reference Category

b **LURIC (nc-APRIL)**

Parameter	Hazard ratio	Lower .95	Upper .95	P values
Log nc-APRIL	1.14	1.02	1.27	0.022
age	1.06	1.04	1.07	0.000
sex	0.70	0.53	0.92	0.011
CRP	1.38	0.95	2.01	0.087
Triglycerides (log)	0.84	0.63	1.12	0.230
Total cholesterol (log)	1.26	0.86	1.85	0.240
Myocardial infarction (no vs one)	1.06	0.82	1.37	0.666
Myocardial infarction (no vs >one)	1.93	1.33	2.81	0.001
Stroke	1.61	1.17	2.22	0.003
Periph. Vasc. Disease	1.83	1.33	2.50	0.000
BMI	0.98	0.95	1.02	0.331
Isolated systolic hypertension (>=140/<90)	0.83	0.65	1.06	0.140
Type II diabetes	1.25	0.89	1.76	0.189
Creatinine (log)	1.86	1.19	2.90	0.007
Hba1c (%)	1.25	1.13	1.39	0.000

c **FAST-MI (nc-APRIL)**

Variable	Multivariate		
	Hazard ratio	CI	P-value
Death or recurrent myocardial infarction			
3 rd Tertile	1.91	1.25-2.91	0.0006
2 nd Tertile	0.77	0.45-1.33	ns
1 st Tertile *	-	-	-

*Reference Category

Extended Data Table 1